universität wien

MASTERARBEIT / MASTER'S THESIS

Titel der Masterarbeit / Title of the Master's Thesis

„Transformations of Cu based nanomaterials in soil“

verfasst von / submitted by

Brigitte Simone Gerstmann, BSc.

angestrebter akademischer Grad / in partial fulfilment of the requirements for the degree of

Master of Science (MSc.)

Wien, 2017 / Vienna 2017

Studienkennzahl lt. Studienblatt / degree programme code as it appears on the student record sheet:	A 066 815
Studienrichtung lt. Studienblatt / degree programme as it appears on the student record sheet:	Masterstudium Erdwissenschaften
Betreut von / Supervisor:	Univ.-Prof. Dr. Thilo Hofmann
Mitbetreut von / Co-Supervisor:	Dr. Adam Laycock

Acknowledgements

First, I would like to thank Adam and Thilo for being such inspiring and supportive supervisors. Many thanks also to Frank and Antonia for sharing their knowledge on single particle data treatment. Further I would like to thank the rest of this vivid working group.
On a personal level, I would like to thank David. Thanks for your support, patience, love and impeccable sense of humor. Thanks also to my family who provided me with roots to grow and wings to fly and to my friends, especially Stephanie & Flora, who have accompanied me throughout the last two years and beyond. Finally, special thanks to my cat Xidi for grounding me.

Declaration of Academic honesty

With my signature, I certify that this thesis has been written by me using only the indicated resources and materials. Where I have presented data and results, the data and results are complete, genuine, and have been obtained by me unless otherwise acknowledged. I further confirm that this thesis has not been submitted, either in part or as a whole, for any other academic degree at this or another institution.

Brigitte S. Gerstmann, November 2017

Summary

Plant protection prevents agricultural losses worth several billion US$ a year (Agrios, 2005). Plant protection products (PPPs) are partly copper (Cu) based due to its biocidal properties and acceptance in organic agriculture. In Austria, approximately 115 tons of these Cu based PPPs were sold in 2008 (Bundesamt für Ernährungssicherheit, 2017). However, the long-term and routine spraying of Cu based PPPs to plants and crops can lead to Cu accumulation in many agricultural soils. This raises growing concern as Cu accumulation affects soil and water quality. One proposed approach to reduce the amount of Cu applied to agricultural land is through the application of nano-enhanced PPPs. Such products may have beneficial properties due to the inclusion of nano sized materials with an increased surface-to-volume ratio. Yet, there are many uncertainties regarding the fate of these materials once they enter the environment.

The aim of this master's project is to investigate the environmental behavior of CuO NPs in soil and to compare the results with conventionally used Cu based PPPs. This was achieved by a 31-day soil incubation study in which LUFA 2.2 standard soil was treated with CuO NPs, three selected commercially available PPPs, or an ionic Cu solution in addition to control incubations. To assess Cu partitioning between the bioavailable and the colloidal soil fraction over time the soils were sampled and processed using a two-step sequential soil extraction procedure: First, a $CaCl_2$ extraction was performed to obtain labile, bioavailable Cu extracts. Second, a 1% FL70 solution, an alkaline detergent, was applied to obtain stable colloidal extracts. These extracts were then analyzed for total Cu and NP number and size using conventional inductively coupled plasma mass spectrometry (ICP-MS) and single particle (sp) ICP-MS, respectively. Although spICP-MS is a powerful tool in NP analysis, signal processing remains a challenging task. Especially, when a sample contains both metal based NPs and dissolved metal ions. Thus, an important part of this master's project was the development of a data processing script. The script was written in R, based on an established statistical test. It was successful in processing the single particle data in a reliable and objective manner.

Regarding the findings, two main trends were identified in total Cu concentrations in the soil extracts: a total Cu decrease over time in soil incubated with PPPs and the control settings and a total Cu increase over time in soil incubated with CuO NPs. The first trend can be attributed to an increased ionic Cu complexation by soil organic matter (SOM) with time.

The second trend is explained by steady ionic Cu release due to NP dissolution. Moreover, Cu containing NPs were successfully detected in the soil dosed with CuO NPs and in one of the soils dosed with commercially available PPPs. The average particle number and size decreased with increasing incubation time while the NP size distribution diagrams shifted to smaller sizes. These NP transformations in size were attributed to particle dissolution.

As Cu accumulation in soils caused by the application of Cu based PPP poses a considerable risk to environmental health, this study contributes to understand the environmental fate of alternative, nano-enhanced PPPs. This further helps to inform the safe design of new products that aim to minimize environmental impact whilst maintaining efficient crop protection. This master's project also contributes to the development of spICP-MS applications by studying Cu based NP transformations in complex natural media over time. Additionally, this project provides a single particle data processing tool that is not only based on an established statistical test, but also available in the free and open-source software R.

Zusammenfassung

Der Einsatz von Pflanzenschutzmitteln verhindert jährlich landwirtschaftliche Verluste in der Höhe von mehreren Milliarden US$. Der Großteil der in der EU verkauften Pflanzenschutzmitteln fällt unter die Kategorie Bakterizide und Fungizide, die zum Teil auf Kupfer (Cu) basieren und auch in der ökologischen Landwirtschaft akzeptiert sind. Zum Beispiel wurden im Jahr 2008 in Österreich etwa 115 Tonnen an Cu-haltigen Pflanzenschutzmitteln verkauft. Kupfer hat jedoch nicht nur biozide Eigenschaften, die der Schädlingsbekämpfung nutzen können, sondern auch die Tendenz, sich im Boden anzureichern. Der langjährige, regelmäßige und intensive Einsatz von Pflanzenschutzmitteln auf Kupferbasis hat daher zu Cu-Anreicherung in vielen landwirtschaftlichen Böden geführt. Ein Ansatz zur Verringerung der gängigen Cu-Aufwandmengen ist die Verwendung alternativer Produkte, die Nanopartikel enthalten. Nanopartikel (NP) können, aufgrund ihrer großen spezifischen Oberfläche, neue Eigenschaften und eine verstärkte Reaktionsfähigkeit aufweisen. Es gibt jedoch auch eine Vielzahl an Unsicherheiten, die das Entlassen solcher Partikel in die Umwelt begleiten.

Ziel dieser Masterarbeit ist daher, das Verhalten von CuO NP im Boden zu untersuchen und mit dem herkömmlicher Produkte zu vergleichen. Dies wurde durch eine 31-tägige Bodenstudie erreicht, in der CuO NP, drei ausgewählte Pflanzenschutzmittel auf Kupferbasis oder zwei Kontrolllösungen (ionisches Cu und deionisiertes Wasser) in LUFA 2.2 Standard-Boden inkubiert wurden. An ausgewählten Tagen wurden Bodenproben entnommen, die anhand eines zweistufigen, sequentiellen Extraktions-Protokolls aufbereitet wurden: Zum einen wurde pflanzenverfügbares Cu durch eine $CaCl_2$ Lösung extrahiert. Zum anderen wurden drei sequentielle Extraktionen mit FL70, einem alkalischen Tensid, durchgeführt, um stabile Colloid-Suspensionen zu erhalten. Die Konzentrationen von gelöstem Cu wurden im Anschluss mit ICP-MS bestimmt und die Kolloid-Extrakte wurden auf NP- Gehalt- und -Größe in Einzelpartikel (sp) ICP-MS untersucht. Obwohl spICP-MS sich zunehmend als Routineanwendung etabliert, bleibt die Signalverarbeitung eine Herausforderung. Insbesondere, wenn die Analyt-Suspension neben Metall-basierten NP zusätzlich das gleiche Metall in gelöster Form enthält.

Ein Hauptaugenmerk dieser Masterarbeit war daher die Datenanalyse. Dazu wurde ein Skript basierend auf einem gängigen, statistischen Test in der Statistik-Software R entwickelt, das die Rohdaten reproduzierbar und objektiv verarbeitet.

Zwei Haupttrends wurden im Verhalten von gelösten, bioverfügbaren Cu identifiziert: Eine Cu-Abnahme mit zunehmender Inkubations-Zeit in den Bodenproben mit den herkömmlichen Pflanzenschutzmitteln und den Kontrolllösungen. Das kann durch die zunehmende Komplexierung von gelöstem Kupfer insbesondere durch das im Boden enthaltene, organische Material erklärt werden. Im Gegensatz dazu wurden steigende Cu-Konzentrationen mit zunehmender Inkubations-Zeit in den Bodenproben mit CuO NP nachgewiesen. Das kann auf das Auflösen der CuO NP und die damit einhergehende, zunehmende Freisetzung von Cu Ionen zurückgeführt werden. Cu-haltige NP wurden im Laufe des Versuches erfolgreich in zwei Bodenproben detektiert: In der Probe mit den CuO NP und in einer mit einem herkömmlichen Pflanzenschutzmittel. Die mittlere Partikelanzahl und –größe nahmen dabei mit zunehmender Zeit ab und die Verteilungsdiagramme verlagerten sich zu kleineren Partikelgrößen. Auch diese Trends weisen auf ein zunehmendes Auflösen der NP im Boden hin.

Das Verhalten und die Transformationen von CuO NP im Boden, im Vergleich mit herkömmlichen Cu basierenden Pflanzenschutzmitteln, bieten neue Erkenntnisse auf potentielle Umweltauswirkungen dieser Materialen. Diese Erkenntnisse können ein Beitrag zum sicheren Design neuer Pflanzenschutzmittel sein, die gängige Cu-Aufwandmengen und –raten in der Landwirtschaft verringern könnten. Zusätzlich leistet diese Masterarbeit einen Beitrag zur Entwicklung von spICP-MS Anwendungen, da NP Transformationen in komplexer Boden-Matrix erfolgreich über 31 Tage bestimmt wurden. Im Rahmen dieser Arbeit wurde auch ein Skript zur Datenverarbeitung (spICP-MS) entwickelt, das nicht nur auf einer anerkannten, statistischen Methode beruht, sondern auch in der gratis und open-source Software R zur Verfügung steht.

List of figures

List of tables

Abbreviations

EC… European Commission

EDX… Energy-dispersive X-ray analysis

EELS… Electron energy loss spectroscopy

EU... European Union

CEC… Cation exchange capacity

DLS... Dynamic light scattering

DOM… Dissolved organic matter

FAO… Food and Agriculture Organization of the United Nations

FFF… Field-flow fractionation

IUPAC ... International Union of Pure and Applied Chemistry

NM... Nanomaterial

NP... Nanoparticle

LUFA… Landwirtschaftliche Untersuchungs- und Forschungsanstalt

PMP… Polymethylpentene

PPP… Plant protection product

ICP-MS… Inductively coupled plasma mass spectrometry

SAED…Selected area electron diffraction

SEM… scanning electron microscopy

SOM… Soil organic matter

Std… Standard deviation

spICP-MS… single particle inductively coupled plasma mass spectrometry

TEM... transmission electron microscopy

UN/UNO… United Nations Organization

WHC… Water holding capacity

WHO… World Health Organization

This page is intentionally left blank

Table of Content

1. Introduction

"End hunger, achieve food security and improved nutrition and promote sustainable agriculture" - These are the aims of the UN development goal *Zero Hunger* which is ranked second among the 17 sustainable development goals for 2030 (UN, 2015). Hence, modern agriculture does not only face the challenge to feed an increasing world population, but also to ensure an intact environment for future generations. One crucial aspect in agriculture is plant protection as it prevents losses worth several billion US$ a year (Agrios, 2005). The most sold group of plant protection products (PPPs) in the EU in 2014 were fungicides and bactericides (> 170 000 tons) representing ~44 % of total PPP sales (Eurostat, 2016).

Some of these products are based on copper (Cu) as active substance due to its biocidal properties and acceptance in organic agriculture. For example, the applied quantities of Cu based PPPs were 320 and 115 tons for Germany and Austria, respectively (Kühne *et al.*, 2009)(Bundesamt für Ernährungssicherheit, 2017). However, the routine application of these Cu-based PPPs in agriculture leads to the accumulation of Cu in soil; thereby posing a considerable threat to soil and water resources. Restrictions on the usage of Cu in agriculture have consequently been implemented by the European Union (European Commission (EC), 2002, 2009b; Rusjan, 2012). This is especially relevant for countries like Austria that has a leading role in organic viticulture in the EU and strongly relies on Cu based PPPs (Berger *et al.*, 2012; Vogl and Hess, 2016).

However, one proposed strategy to reduce the Cu loads applied to agricultural land whilst maintaining PPP efficiency is the application of nano-enhanced PPPs. Such products present a promising alternative to the conventional PPPs on the market due to the increased surface area to volume ratio of nanoparticles (NPs). Yet, there is much uncertainty regarding the fate of NPs once released into the environment (Gogos *et al.*, 2012; Kah and Hofmann, 2014; Kookana *et al.*, 2014; Kah, 2015). As the spraying of nano-enhanced PPPs to plants and crops will inevitably lead to the addition of pristine NPs to soil, it is crucial to understand their environmental behavior and fate. To do so, first analytical techniques are needed that are capable of detecting and characterizing engineered NPs in complex soil matrix at typical low environmental levels.

One technique with such a potential is single particle Inductively Coupled Mass Spectrometry (spICP-MS) (Degueldre and Favarger, 2003; Pace, Nicola J. Rogers, *et al.*, 2012;

von der Kammer *et al.*, 2012; Majedi and Lee, 2016). Despite the analytical capabilities however, detecting metal based NPs in natural samples remains a challenging task. Besides issues regarding sample preparation, a major challenge is data processing to distinguish signals from NPs and from dissolved ions (Tuoriniemi *et al.*, 2012; Cornelis and Hassellöv, 2014; Navratilova *et al.*, 2015).

1.1 State of knowledge

1.1.1 Behavior of Cu in soil

From ancient tools and jewelry to modern electronic technology, copper (Cu) has become an indispensable element for human civilization with a considerably growing demand (Elshkaki *et al.*, 2016). The transition metal with the atomic number 29 occurs naturally in two stable isotopes ^{63}Cu and ^{65}Cu with relative abundances of 69,15% and 30,85%, respectively (IAEA, 2010).

Besides its metallic state, Cu exists in oxidation states of -2, +1, +2, +3 and +4. In soil, Cu occurs predominantly in the divalent form (Cu^{2+}) (Mengel *et al.*, 2001). This is illustrated by

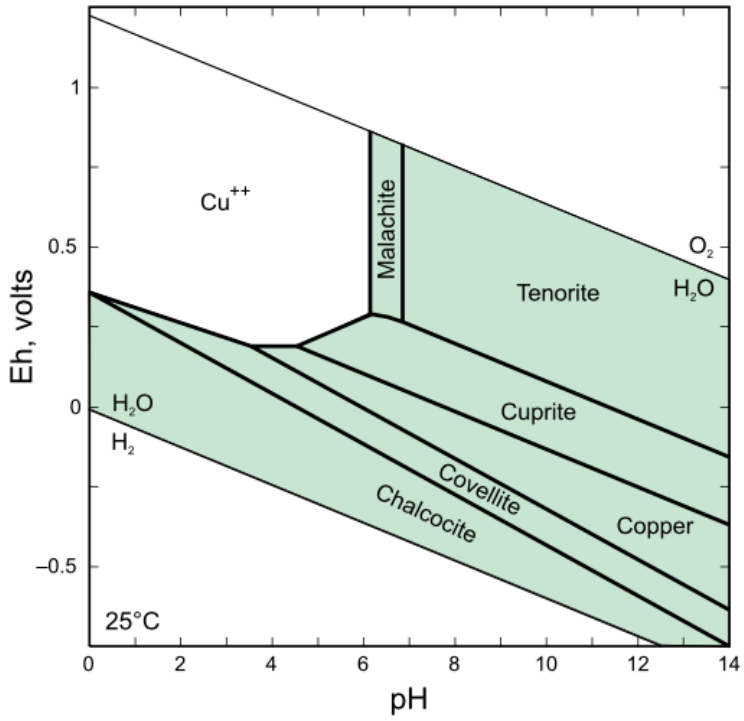

Figure 1: Eh-pH diagram for copper with the stability field of Cu^{2+} in moderately to highly oxidizing conditions and at pH < 6. (T = 25°C, total inorganic carbon = 10^{-2} mol kg^{-1}, total Sulphur = 10^{-3} mol kg^{-1} and total Cu = 10^{-5} mol kg^{-1} (Retrieved from Ford & Wilkin, US-EPA (2010)).

Figure 1 where the Cu^{2+} stability field occurs at pH < 6 and in moderately to highly oxidizing systems, such as soil. The other Cu species illustrated are the Cu hydroxylcarbonate Malachite ($Cu_2CO_3(OH)_2$), the Cu oxides Tenorite (CuO) and Cuprite (Cu_2O), elemental copper (Cu^0) as well as the Cu sulfides Covellite (CuS) and Chalcocite (Cu_2S) (Ford and Wilkin, 2010). Hence, the prevalence of Cu^{2+} can change under fluctuating redox conditions causing Cu reduction and potentially the precipitation of metallic Cu or Cu sulfides (Weber *et al.*, 2009). The Cu levels in European topsoil range from 0,81 to several hundred mg kg^{-1} and depend on the parent material from which the soil was formed and potential Cu contamination (Mengel *et al.*, 2001; Salminen, 2005). In uncontaminated soils, the highest proportion of Cu is contained within the crystal lattices of primary (e.g. Chalcopyrite) or secondary minerals (e.g. Malachite). The presence of ionic Cu^{2+} in soil solution is limited by its sorption affinity: A large fraction of Cu is sorbed to the immobile soil matrix including inorganic constituents (e.g. phyllosilicates, Al-, Fe- or Mn- hydroxides) and soil organic matter (SOM). In comparison to other divalent cations, Cu has a considerably strong affinity to SOM, as shown by the following sequence:

$$Cu > Ni > Pb > Co > Ca > Zn > Mn > Mg$$

In SOM it is either chelated by coordinative bonding to O, N and S or by covalent bonding to the carboxylic groups of humic or fulvic acids. (Mengel *et al.*, 2001; Sposito, 2008).

Besides the immobile soil matrix, Cu may also be associated with the mobile soil fraction. In this fraction, both organic and inorganic soil constituents are present in the form of colloids that may sorb Cu to their surfaces. The presence of such colloids is thereby likely to enhance Cu mobility in the subsurface (McCarthy and Zachara, 1989; Pauwels *et al.*, 2002; Grolimund and Borkovec, 2005). Mobile and immobile inorganic soil compartments (e.g. Fe oxides) may additionally be coated with negatively charged organic acids that further promote metal sorption (Kretzschmar and Sticher, 1997). The soil pH affects the degree of Cu sorption to particle surfaces as H^+ ions may compete for the same sorption sites (Mengel *et al.*, 2001).

Yet, soil parameters like pH, cation exchange capacity (CEC) and SOM content do not only govern the mobility of Cu in soil, but also its availability to biota (van Gestel, 2008; Lu *et al.*, 2009; Rusjan, 2012). Cu bioavailability in soil is crucial as Cu is an essential micronutrient

that takes part in numerous physiological processes of living organisms (Mengel *et al.*, 2001; Rusjan, 2012). On the other hand, a Cu surplus in soil, relative to natural background concentrations, may act phytotoxic by damaging cell functions in plants, and may provoke measureable toxicological responses in soil invertebrates and microbial communities (Mengel *et al.*, 2001; Komárek *et al.*, 2010; Bundesamt für Ernährungssicherheit, 2017).

One of the input pathways of this excess Cu in soil is the spraying of Cu containing PPPs in agriculture. The biocidal properties of Cu have been known since the mid 19th century and have been used to combat fungal and bacterial plant infections, such as Downy mildew (*Plasmopara viticola*). More recently, Cu-based PPPs gained special popularity due to their acceptance in organic agriculture (FAO, 1999). The form of Cu used in commercially available PPPs include copper sulphate ($CuSO_4$), copper oxychloride ($Cu_2Cl(OH)_3$), copper hydroxide ($Cu(OH)_2$) and cuprous oxide (Cu_2O). However, the spraying of these products is a well-known cause for Cu accumulation in agricultural soils and thereby poses a considerable threat to environmental health (Ma *et al.*, 2006; Rusjan *et al.*, 2007; Lu *et al.*, 2009). A proposed approach to reduce dosing levels is the usage of nano-enhanced PPPs (Servin *et al.*, 2015).

1.1.2 Cu based NPs in soil

Over the last decade, PPPs incorporating nanomaterials (NMs) have been developed (Kah, 2015). These nano-enhanced PPPs aim to increase PPP efficacy while requiring less material and thus, keeping the environmental impact at a minimum (Servin *et al.*, 2015). This is achieved by making use of the increased surface area to volume ratio of NPs relative to the same bulk materials in coarser grain sizes (Kah and Hofmann, 2014; Kah, 2015; Servin *et al.*, 2015). Nevertheless, potential benefits like an increased efficacy, durability and hence reduced application levels and rates come along with many uncertainties regarding environmental fate that are yet to be addressed (Gogos *et al.*, 2012; Kah and Hofmann, 2014; Kah, 2015). In soil media, many physical and chemical factors like soil texture, fracturing, soil water regime and chemistry including soil pH and ionic strength, as well as SOM and mobile organic and inorganic phases may all influence NP fate (Cornelis *et al.*, 2014).

Nano-enhanced PPPs that are Cu based were reported to incorporate the same bulk materials as conventional PPPs, yet in form of NPs. Examples are NPs made from metallic Cu

(Cu^0), Cu oxides (CuO/Cu_2O), and Cu hydroxides ($Cu(OH)_2$) (Giannousi *et al.*, 2013; Tegenaw *et al.*, 2015). Based on soil solution chemistry, it has been demonstrated that Cu added to soils as CuO NPs ages differently to Cu derived from dissolved Cu salts in soil with time (McShane *et al.*, 2014; Gao *et al.*, 2017). Gao et al., 2017 documented this difference by studying extractability of bioavailable Cu in soil with time. While Cu bioavailability in soil dosed with the Cu salt decreased rapidly with increasing incubation time, Cu bioavailability steadily increased in the soil dosed with CuO NPs. These differences were attributed to time-dependent Cu release caused by NP dissolution.

Processes like NP dissolution lead to NP transformations that affect the long-term fate of these materials (Lowry *et al.*, 2012). An approach to assess these transformations could be the investigation of NP number and size in soil over time.

1.1.3 Detection of Cu based NPs in soil

Detection of engineered NPs in soil is a challenging task due to the coexistence of a variety of dissolved species, soil colloids and bulk solids that may contain the same element and/or be in the same size range. A variety of detection methods is available, yet, each having their own restraints. Exemplary common methods for NP detection and analysis are, beside many others, scanning and transmission electron microscopy (SEM/TEM), dynamic light scattering (DLS) and single particle Inductively Coupled Mass Spectrometry (spICP-MS) (von der Kammer *et al.*, 2012; Xing *et al.*, 2016).

Physical size fractionation of a sample can be achieved by methods like centrifugal separation, ultrafiltration, size exclusion chromatography (SEC) or Field-flow fractionation (FFF). Centrifugation and ultrafiltration aim to separate NPs from larger particles and dissolved species. In centrifugation, NPs are separated from a supernatant by sedimentation whereas in ultrafiltration, NP size separation is achieved by a hydrostatic force that is applied to a membrane (Majedi and Lee, 2016). Total metal concentrations of size fractions can then be determined by digestion, for example. Yet, sample digestion does not yield information on the particle size, shape or composition (Xing *et al.*, 2016). In SEC the porous medium retains NPs depending on their size, shape and density. This method yields good separation efficiency, nevertheless disadvantages are a narrow size range and possible interactions between the sample and the stationary phase (Tiede *et al.*, 2008).

FFF is a versatile family of techniques in which an external field is applied to a sample that first hits a membrane (accumulation wall) and then moves along an open channel. Different modes and flow regimes may be applied, yet its basic principle is the hydrodynamic separation of NP fractions based on different diffusion coefficients. The diffusion coefficients depend on NP properties (e.g. NP size, molecular weight, charge etc.) and govern the retention/elution time of NP fractions (Baalousha *et al.*, 2011; von der Kammer *et al.*, 2011; Majedi and Lee, 2016). Coupled with detectors like ICP-MS, this method can offer information on chemical composition across a size distribution for example (von der Kammer *et al.*, 2011). However, relative to other methods, this powerful technique is still sophisticated in practice as sample preparation is substantial to avoid interferences of larger particles and as several operational aspects like flow regime, field-strength and channel geometry need to be optimized to achieve robust separation (Dubascoux *et al.*, 2008; von der Kammer *et al.*, 2011). This is crucial as NP type and size as well as NP interactions with each other and/or the FFF membrane (channel wall) can affect the elution time of NP fractions. Additionally, pre-concentration of samples at low particle concentrations may be required before analysis (Majedi and Lee, 2016).

The common imaging and analytical techniques SEM and TEM can be used to determine particle size distributions. Both techniques can be additionally coupled with analytical tools to resolve elemental compositions of a given sample. Examples for such analytical tools are Energy-dispersive X-ray analysis (EDX) that can be combined with both SEM and TEM and Electron energy loss spectroscopy (EELS) that can be coupled with TEM. Yet, EDX and EELS yield quantitative uncertainties of ~20 % and ~10 %, respectively. Information on crystalline properties of NPs can be obtained through selected area electron diffraction (SAED) coupled with TEM, for example (Mavrocordatos *et al.*, 2004). Nonetheless, SEM and TEM are capable of imaging primary NPs and NPs within larger aggregates, but are prone to artefacts from sample preparation. Additional errors may occur as sizes of 3D objects are determined via 2D images. Furthermore, large NP numbers ($n > 30$) need to be counted for a representative (normal) distribution of NP sizes in a sample (Barlow, 1989; Tiede *et al.*, 2008). Hence, sizing, counting and likely sole identification of engineered NPs is challenging at environmentally relevant quantities within polydisperse and heterogeneous soil samples.

DLS is a widely used technique that yields particle size distributions based on Brownian motion and light scattering of NPs. It is user-friendly but strongly biased towards larger

particles with higher scattering intensity. Additionally, DLS is not able to distinguish NP sizes within aggregates and limited to rather homogeneous size distributions with a low polydispersivity index (Xing *et al.*, 2016).

A promising technique able to analyze single particles within complex media and at low concentrations typical for environmental samples is spICP-MS (Tuoriniemi *et al.*, 2012; von der Kammer *et al.*, 2012; Majedi and Lee, 2016). Since the determination of NP sizes is based on an assumed particle composition and an assumed spherical shape, a sample should ideally contain NPs with known composition, well-characterized shape and sizes that are detectable above a dissolved baseline. Since the latter is rarely the case in natural samples, many authors emphasize the importance of accurate and objective data processing to distinguish between signals from dissolved ions and NPs (Laborda *et al.*, 2011; Tuoriniemi *et al.*, 2012; Cornelis and Hassellöv, 2014; Navratilova *et al.*, 2015). Navratilova et al. (2015) demonstrated the applicability of spICP-MS in detecting CuO NPs in soil colloidal extracts and processed the raw data based on a statistical outlier test adapted after Tuoriniemi et al. (2012). However, the study by Navratilova et al. (2015) focused on optimizing NP detectability at a high dissolved background. To achieve this, soil colloidal extracts were prepared first, spiked with pristine CuO NPs and then analyzed with spICP-MS. According to the authors, their study neither addressed CuO NPs directly added to soil nor a time dependency which presents a more realistic scenario and thus, a current research gap.

1.2 Research scope

Whereas the aging of Cu derived from CuO NPs in soil has been investigated, limited knowledge is available on time-dependent transformations of the NPs in soil and the difference in behavior relative to conventional Cu based PPPs (McShane *et al.*, 2014; Gao *et al.*, 2017). This project aims to investigate these transformations and differences in a soil incubation study over 31 days. To accomplish this, spICP-MS is applied for particle characterization and conventional Inductively Coupled Mass Spectrometry (ICP-MS) for dissolved Cu measurements. Additionally, a script was written in the statistical programming language R to enable objective processing of the spICP-MS raw data. The partitioning of Cu between the colloidal and the dissolved soil fractions was then studied over time and comparisons drawn between CuO NPs and conventional PPPs to gain information on the environmental fate of these materials.

1.3 Terms and Definitions

Active substance: As defined by the European Commission (EC), an active substance is "*any chemical, plant extract, pheromone or micro-organism (including viruses) that has action against 'pests' or on plants, parts of plants or plant products*" and requires a safety approval by the EC before being used within a plant protection product (European Commission (EC), 2016). The usage of Cu as active substance is in accordance with both organic farming practices and EC safety requirements within copper hydroxide, copper oxychloride, copper sulphate and copper oxide (European Commission (EC), 2009b, 2017).

Bioavailability: Bioavailable ions may be defined as dissolved or loosely bound ions in soil that are readily available for plant uptake (Shuman, 1991; Sposito, 2008; Hooda, 2010). Note that throughout this study, the term "bioavailable Cu" is used interchangeably with "labile Cu". Both refer to dissolved, ionic Cu exclusively.

Colloid: According to IUPAC a colloid, short for colloidal system, refers to "*a state of subdivision such that the molecular and polymolecular particles dispersed in a medium have at least one direction or dimension roughly between 1 nm and 1 µm, or that in a system discontinuities are found at distances of that order*" (Everett, 2009).

Nanomaterial (NM): According to the definition recommended by the EC, a nanomaterial means "*a natural, incidental or manufactured material containing particles, in an unbound state or as aggregate or agglomerate and where 50 % or more of the particles in the number size distribution, one or more external dimensions is in the size range 1nm-100 nm*", whereas "(..) *in specific cases where warranted by concerns for the environment, health, safety or competitiveness the number size distribution threshold of 50% may be replaced by a threshold between 1 and 50 %.*"(European Commission (EC), 2011, 2013; Gottardo *et al.*, 2017). Nevertheless, this definition is based on size as the only defining property, mainly for regulatory purposes. Whether novel properties exhibited specifically by materials in nano size range (1-1000 nm) should be involved in a definition is still subject to ongoing scientific and regulatory debate (Kah *et al.*, 2013; Kah and Hofmann, 2014; Gottardo *et al.*, 2017).

Nanoparticle (NP): A *nanoparticle* is hence a derivative of a *nanomaterial* and a *particle* is defined as a "*minute piece of matter with defined physical boundaries*" (European Commission (EC), 2011).

Nano-enhanced PPP: This term is used in this study to describe plant protection products that, as defined by (Kah and Hofmann, 2014), "*(i) Intentionally include entities in the nm size range (1-1000 nm), (ii) are designated with a "nano" prefix (..), and/or (iii) are claimed to exhibit novel properties associated with the small size of their components*"

Organic agriculture: Various definitions and certification programs exist for this term. However, the FAO/WHO (1999) summarizes as follows: "*Organic agriculture is a holistic production management system which promotes and enhances agro-ecosystem health, including biodiversity, biological cycles and soil biological activity. (..) This is accomplished by using, where possible, agronomic, biological, and mechanical methods, as opposed to synthetic materials, to fulfill any specific function within the system.*" The elementary rule in this understanding of organic farming is that synthetic inputs are prohibited and natural (not-synthetic) inputs are accepted. These natural inputs comprise organic substances created by naturally occurring biological processes (e.g. manure) or inorganic substances that are not chemically altered from their mineral source (e.g. inorganic Cu compounds) (FAO, 1999; Vogl and Hess, 2016).

Plant protection product (PPP): As defined by the EC PPPs *"protect crops or desirable or useful plants"* (European Commission (EC), 2016). They contain at least one active substance that either acts as i) crop protection against pests, diseases or growth of undesired plants/parts of plants or ii) regulator of life processes such as plant growth.

2. Materials & Methods

This chapter provides details on the test materials and reagents (2.1) and on the lab equipment and instrumentation used (2.2). Subsequently, the initial characterization of the test materials (2.3), the soil incubation protocol (2.4), the sampling and sample preparation (2.5) are outlined. The final section describes the analytics and data processing (2.6) that were involved in this soil incubation study.

2.1 Test materials and reagents

2.1.1 Standard soil

The standard soil LUFA 2.2 was used as incubation matrix and purchased from LUFA (Landwirtschaftliche Untersuchungs- und Forschungsanstalt) Speyer in Germany. The natural soil classifies as loamy sand and originates from 0-20 cm of depth. A carbon content of 1,61 ± 0,15 wt. % and a pH-value of 5,4 (0,01 M $CaCl_2$) were reported by LUFA Speyer. It was sieved using a 2-mm filter screen before shipping and air-dried prior to the experiments. Soil samples of 150 g were placed into acid-leached Polymethylpentene (PMP) containers and subsequently spiked with the dosing solutions or suspensions containing CuO NPs, selected commercially available PPPs or controls.

2.1.2 CuO NPs

In this study, CuO NPs were purchased from Sigma Aldrich. The material is sold as Copper (II) Oxide (Cupric oxide) powder with an average particle size of 50 nm based on TEM. Details on the CuO NP stock suspension that was prepared for soil dosing are listed in Table 1. This stock suspension (33 ml) was then dosed to one of the soil samples (150 g) to achieve a Cu concentration of 100 mg kg^{-1} dry soil and a moisture content of 21 %, equivalent to 50% of the water holding capacity (WHC).

2.1.3 Commercial Cu-based PPPs

The commercially available PPPs Bordeaux, Cupravit and Kocide were selected for this study. They all have Cu as their active substance and their usage in agriculture is approved within the EU (European Commission (EC), 2017). The products were supplied by the University of Aveiro, Portugal. Stock suspensions for soil dosing were prepared for each

material. Table 1 shows the proportion of Cu in each formulation, the mass and the volume of Milli-Q water required for a target concentration of 0,45 mg ml^{-1}. Soil samples à 150 g were then dosed with 33 ml of these suspensions to achieve soil dosing at a Cu concentration of 100 mg kg^{-1} dry soil. Further information on the soil dosing procedure can be found in section 2.4.

Bordeaux mixture (Copper sulfate and Calcium Hydroxide) is named after its place of invention and has been used since the mid 19^{th} century against various fungus diseases (Berger *et al.*, 2012; Rusjan, 2012). Chemically, it is a combination of the Cu salt $CuSO_4$ and Calcium hydroxide $Ca(OH)_2$ and will be referred to as Bordeaux hereafter. In Austria, the usage of Bordeaux is no longer approved (Patnaik, 2003; Bundesamt für Ernährungssicherheit, 2017)

Cupravit (Copper Oxy-chloride) by Bayer is a Cu based PPP with the chemical formula $Cu_2Cl(OH)_3$ (European Commission (EC), 2009a). In Austria, Copper Oxychloride is generally authorized, yet the trademark Cupravit is not registered (Bundesamt für Ernährungssicherheit, 2017).

Kocide 3000 (Copper Hydroxide) by Dupont is composed of 46,1 % Copper Hydroxide $Cu(OH)_2$ and 53,9 % inert material (Certis USA, 2017). The application of Copper Hydroxide is authorized in Austria and according products are registered the Austrian database for approved PPPs. However, the trademark Kocide is not included (Bundesamt für Ernährungssicherheit, 2017). This material will be referred to as Kocide hereafter.

2.1.4 Control settings

Two control settings were studied simultaneously to exclude that i) elevated dissolved Cu levels and ii) the presence of naturally occurring particles in the standard soil yield detectable NPs. A dissolved Cu solution and pure Milli-Q were therefore spiked to standard soil samples and are referred to as ionic Cu and as blank control, respectively.

Ionic Cu control ($CuSO_4$): Copper sulphate (also known as cupric sulphate, blue vitriol, blue copperas or blue stone) is a water-soluble Cu salt. Copper sulphate has a history of

agricultural usage and is most prominently an ingredient of Bordeaux Mix (section 2.1.3) (Patnaik, 2003).

The material was purchased as Copper (II) Sulfate pentahydrate from Merck and was used to create a dissolved Cu control solution. The amounts of Copper sulphate used in the preparation for the dosing solution is listed in Table 1. This solution was incubated in soil to verify that an elevated dissolved Cu level does not cause the formation of detectable Cu based NPs.

Blank Control (Milli-Q water): In this control setting, 33 ml of Milli-Q water were spiked and incubated in one of the standard soil samples. The aim was to determine the natural bioavailable Cu content of the soil and to exclude the possibility of naturally occurring Cu containing NPs that may result in detectable NPs.

Table 1: Test material amounts in the stock suspensions. Each material was suspended in Milli-Q water at a Cu target concentration of 0,45 mg ml^{-1}. A volume of 33 ml of each suspension was then dosed to a soil sample of 150 g to achieve Cu concentrations of 100 mg kg^{-1} dry soil and a moisture content of 21 % which corresponds to a WHC of 50 %.

Test material	Cu weight fraction [%]	Mass [mg]	Added Milli-Q [ml]
CuO NPs	80	18,2	40
Bordeaux	30	82	50
Cupravit	50	42	46,3
Kocide	30	65,6	43,3
Ionic Cu control	25	72,8	40,7

2.1.5 Reagents

$CaCl_2$ was purchased from Sigma Aldrich as calcium hydrate dihydrate and used for the preparation of 0.1 M $CaCl_2$ solution to extract bioavailable Cu from soil. The alkaline detergent FL70 from Fisher scientific was used to create a 1 % FL70 matrix for particle suspensions and the colloidal extraction step. H_2O_2 from Merck was used to remove organic compounds from samples prior total Cu measurements. Concentrated HNO_3 (65 %) from Merck was purified in a subboiling unit (3 x distillation) and used throughout the study as well as ultrapure water (Milli-Q) with a purity of 18,2 MΩ cm.

2.2 Lab equipment and instrumentation

The entire study was conducted in the Laboratories of the Department of Environmental Geosciences, University of Vienna, Austria. Equipment used was the following: a sonication bath (Sonorex super RK 106, Bandaline, Germany), a shaking table (GFL 3018, Germany), a centrifuge (Jouan CR4.22, Fisher Scientific, USA), a pH-meter (WTW pH 315i, Xylem Analytics, Germany) with a SenTix 81 pH electrode that was calibrated prior measuring, an ICP-MS (7900 ICP-MS, Agilent Technologies, USA) with Ar as carrier gas and Rh as internal standard and a Milli-Q system (Purelab Chorus, Elga, UK) with a quality of 18,2 MΩ cm supplying Milli-Q throughout.

Lab routine: To prevent trace metal contamination, all lab utensils were either acid-leached with 2% HNO_3 for a minimum of 24h, rinsed with Milli-Q and dried (centrifuge tubes, syringes, PMP containers) or rinsed 3 x with Milli-Q (pipette tips) prior usage. The pH-meter was calibrated on each measuring day before measuring the soil pH in the $CaCl_2$ extracts.

2.3 Initial characterization of the test materials

To evaluate whether NPs are contained in the pristine products, and to potentially derive their particle sizes, the test materials were suspended in a 1 % FL70 solution and sonicated for 10 minutes in a sonication bath. Samples were then diluted by 200 times and analyzed by spICP-MS. The results of this initial characterization are presented in section 3.1.

2.4 Soil incubation protocol

Seven soil samples of ~150 g dry weight each were placed into acid-leached PMP containers and amended with different test materials comprising CuO NPs, Bordeaux, Cupravit, Kocide and an ionic and blank control. A graphical summary of this soil dosing procedure is given in Figure 2. First, stock suspensions or solutions with a Cu concentration of 0,45 mg ml^{-1} were prepared for all test materials, with exception of the blank control where Milli-Q was used instead. Details on these stock suspensions are listed in Table 1 in section 2.1. Second, a volume of ~ 33 ml stock suspension was added dropwise to the soil samples under thorough mixing. This volume was chosen to achieve both the target Cu content of 100 mg kg^{-1} dry soil (except blank control) and a soil moisture of 22%. Based on previous experimental work it was assumed that ~1 % moisture would be lost due to the soil

mixing. This was confirmed by a final moisture content of 21% corresponding to 50% WHC. After soil amendment, the soils were weighed to confirm appropriate dosing. Subsequently, the containers were covered with perforated parafilm to enable gas exchange whilst minimizing moisture loss to maintain constant conditions. The containers were then stored in the dark at room temperature. The moisture content of 21 % was maintained throughout the study period by compensating soil moisture loss, based on weight changes, with an according volume of Milli-Q water.

On days 0, 2, 4, 8, 14, 21, and 31 after dosing, soil samples were taken in triplicates and processed using a two-step sequential extraction technique. The resulting soil extracts were analyzed for total dissolved Cu and extractable NP number and size by conventional and spICP-MS, respectively.

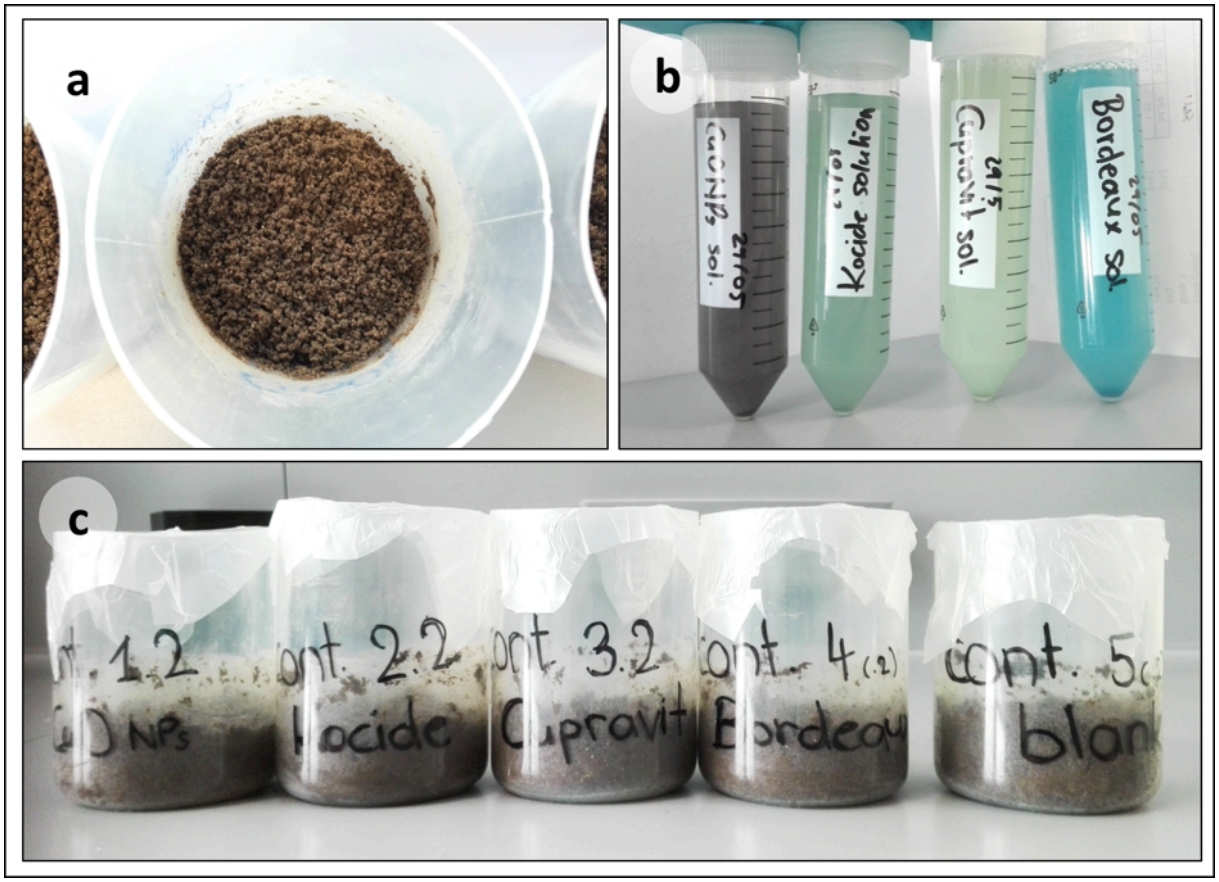

Figure 2: Graphical summary of the soil incubation protocol. ***(a)*** *Air-dried standard soil samples (~150 g each) were spiked with* ***(b)*** *dosing suspensions (~33 ml) containing CuO NPs, Kocide, Cupravit or Bordeaux, accompanied by ionic Cu and blank control solution settings (not all pictured).* ***(c)*** *The soils were incubated over 31 days at constant moisture (21%) at room temperature in dark and sampled on selected days.*

2.5 Sampling and sample preparation

On days 0, 2, 4, 8, 14, 21 and 31 of the incubation period, each soil treatment was sampled in triplicates à 4 g. These samples were processed using a two-step sequential soil extraction procedure: First, a 0,1 M $CaCl_2$ extraction was performed to obtain the dissolved, particle-free Cu fraction (2.5.1). Second, three sequential colloidal extractions were performed using a 1 % FL70 solution (2.5.2).

2.5.1 Bioavailable Cu: 0,1 M $CaCl_2$ extraction

One of the standard methods to determine the bioavailable fraction of an element in soil, is the soil extraction procedure based on $CaCl_2$ solution (Rao *et al.*, 2008). To perform this extraction procedure, 40 ml 0,1 M $CaCl_2$ was added to each 4 g soil sample in 50ml centrifuge tubes. These suspensions were homogenized on a shaking table (type GFL 3018) at 200 rpm for 30 min and centrifuged at a speed of 4007 g for 10 min to separate the sediment from the supernatant. The supernatant was subsequently decanted, its pH-value determined and the absence of NPs confirmed by spICP-MS. The samples were then acidified to 2% HNO_3 and stored in the refrigerator. Finally, the concentration of bioavailable Cu in all $CaCl_2$ extracts was measured using ICP-MS (further described in section 2.6.1).

Besides the extraction of bioavailable Cu, this $CaCl_2$ treatment was likewise adapted in this study to remove suspended NPs from solution. The elevated ionic strength (0,1 M $CaCl_2$ used instead of 0,01 M) induces particle aggregation and the resulting aggregates are removed by centrifugation. This consideration is based on the Schulze-Hardy rule which defines the destabilization of a given suspension by the coagulation of particles as a function of counterion valence. A high ionic strength of a given particle suspension compresses the width of the electric double layer (surrounding the charged particle surfaces) and promotes particle aggregation (Nowicki and Nowicka, 1994). Once aggregated, the NPs will be separated along with the sediment during centrifugation due to the increased mass of the aggregate. The complete removal of NPs from the $CaCl_2$ supernatant was verified by spICP-MS analysis, as no NPs were detected in these extracts.

2.5.2 Colloidal suspensions: 1 % FL70 Colloidal Extractions

In contrast to the previous extraction step, where an extraction of dissolved ions was achieved, this second extraction procedure produced stable colloidal suspensions, which were appropriate for spICP-MS analysis. To achieve this, an extraction reagent of 1% FL70 solution was prepared. FL70 is an alkaline detergent that is commonly used in Field-Flow-Fractionation (FFF) as a colloid carrier. Due to its chemical characteristics, such as an alkaline pH and containing surfactants like EDTA, FL70 is expected to inhibit particle dissolution and aggregation. The samples were prepared using the following protocol: 20 ml 1% FL70 solution were added to the same ~4g of soil sample from the first extraction step. This was followed by homogenizing the mixture on the shaking table for 20 minutes at 200 rpm. The resulting suspension was centrifuged for 1 min at 2424 g rpm to achieve a particle size cut-

Figure 3: Sample preparation steps of sequential soil extractions (performed on day 0, 2, 4, 8, 14, 21 and 31). ***a)*** *Soil treatments (not all pictured)* ***b)*** *Each treatment was sampled in triplicates of 4g* ***c)*** *Reagents were added to the soil samples and homogenized suspension obtained by shaking table* ***d)*** *After centrifugation, the supernatant (above red marks) was decanted and analyzed* ***e)*** *Sequential extracts of one triplicate: one dissolved Cu extract and 3 colloidal extracts with decreasing particle density (from left to right).*

off at 500 nm. The supernatant obtained appeared turbid, reflecting a suspended particle load (Figure 3d). After decanting, 100 µl were removed from each particle suspension and diluted by either 200 x (NPs) or 100 x (PPPs and controls). A volume of ~1 ml was then filtered (0,45 µm) to remove buoyant soil artefacts and analyzed by spICP-MS. The remaining suspension volume was acidified to 5 % HNO_3 and stored in the refrigerator for later total Cu analysis. The colloidal extraction procedure was repeated 3 x for each soil sample. This was done to achieve a gradient of decreasing colloid density in suspension.

2.6 Analytics

The analytics to resolve Cu partitioning between the dissolved ionic and the particulate colloidal phase, comprised conventional (2.6.1) and single particle ICP-MS (2.6.2), respectively and are described below.

2.6.1 Conventional Inductively Coupled Plasma Mass Spectrometry (ICP-MS)

Conventional ICP-MS is an analytical technique to measure element concentrations at trace levels. In this method, a dissolved analyte is transformed into an aerosol and further atomized, ionized by a plasma source, the resulting ions are accelerated and separated according to their mass/charge ratios. The separated ion beam of a target ion is then measured at the detector, usually resolved in millisecond dwell times. The result is a constant intensity signal over time (Figure 4). This signal is then calibrated against a series of standard solutions across a range of known concentrations, any drifts in sensitivity may be monitored and corrected via an internal standard of known concentration (e.g. Rh), to ultimately quantify the total ion concentration in a sample (Thomas, 2001).

Figure 4: Schematic illustration of conventional ICP-MS. Dissolved ions yield a constant signal at the detector, usually resolved in millisecond dwell time.

This conventional ICP-MS set-up was used to determine total Cu in the acidified $CaCl_2$ extracts and acidified colloidal extracts. The latter were first diluted from initially 5 % to a 2 % HNO_3 matrix. All samples were then diluted to a trace concentration of approximately 25 ng ml^{-1} in a 2% HNO_3 matrix before being introduced into the device (7900x ICP-MS, Agilent Technologies, CA, USA) via an auto-sampler.

2.6.2 Single Particle Inductively Coupled Plasma Mass Spectrometry (spICP-MS)

In contrast to conventional ICP-MS, where a constant dissolved ion signal is acquired, single particle mode detects time-resolved intensity spikes of a selected element in the µs-range. These spikes result from the atomization and ionization of single particles. The spike intensity and frequency relates to the particle size and number concentration, respectively. However, the presence of dissolved ions of the same mass yield a background signal that elevates the NP peak (Degueldre and Favarger, 2003), as it is illustrated in Figure 5. In this study, spICP-MS was applied to the colloidal soil extracts (section 2.5.2). The single particle specific set-up comprised a syringe-pump inlet that was operated at a flow rate of 5 µl min^{-1} and a total-consumption nebulizer to increase instrumental NP throughput (transport efficiency). The colloidal extracts were analyzed using 100 µs dwell time and diluted 100 x (PPPs, controls) or 200 x (NPs) prior to analysis. These dilutions were performed to ensure multiple particles are not ionized at the same time.

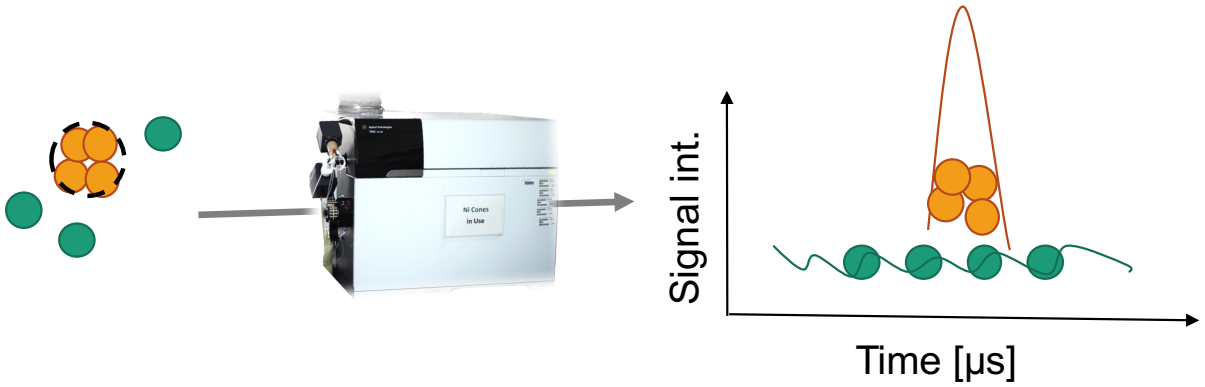

Figure 5: Schematic illustration of spICP-MS. Ionized NPs yield an ion cloud and a signal spike at the detector (orange). The presence of dissolved ions of the same mass elevate the peak above a dissolved baseline.

2.6.3 Single particle data processing in R

The raw data obtained from spICP-MS comprised 10 000 data points per second and included both Cu signals from ionized NPs and from a dissolved ionic Cu background (Figure 5). To discriminate between these two signal types and to reduce the data quantively, the

raw data was treated in the statsistics software R, version 3.3.2 (R, 2016). The according R script (see Appendix, section H) was written in RStudio (Inc. Version 1.0.136 ©2009-2016) using the library library tidyverse (version 1.1.1) with ggplot2 as a plotting tool (Hadley Wickham, 2017).

The flow chart in Figure 6 outlines the data processing steps of the R script. In the first part of the script, the removal of the dissolved Cu baseline from the raw data is achieved by an iterative statistical outlier test. In the second part, the remaining NP intensities are converted into NP sizes. The total intensity (I_{tot}) of a given data point is considered as the sum of the particle intensity ($I_{particle}$), the dissolved Cu baseline intensity (I_{diss}) and an error term (ε).

$$I_{tot} = I_{particle} + I_{diss} + \varepsilon \quad (1)$$

ε describes the analytical error as well as additional errors from machine flickering and/or clocking and was neglected throughout this thesis (as this would go beyond the aims of this Master's project). An iterative statistical outlier test was adapted after Tuoriniemi et al., 2012.

According to the authors, the dissolved Cu background signal is assumed to follow a Normal distribution, whereas the particle signal is assumed to follow a Poisson distribution (Tuoriniemi *et al.*, 2012). The outlier test first defines the mean intensity (μ) and standard deviation (σ) of the data set. Subsequently, a threshold intensity (I_{tresh}) is defined based on these parameters:

$$I_{tresh} = \mu + n\,\sigma \quad (2)$$

I_{tresh} is the sum of the average background intensity μ plus n times (where n = 3, 5) the standard deviation (σ). Data points exceeding this threshold present statistical outliers and are discarded from the data set. This is iteratively repeated until no further statistical outlier can be removed. Hence, this test classifies the raw data into two subgroups: the statistical "inliers" representing the dissolved Cu background and the statistical "outliers"

representing the NP data. Applying 3σ and 5σ thresholds results in confidence intervals of 99,7% and 99,9994 %, respectively. Thus, assuming a normal distribution for the dissolved background, either 1 out of 400 000 data points or 1 out of 1,7 million data points is likely to be assigned to the wrong subgroup. Whereas applying a 3σ threshold is sufficient for samples with a low dissolved metal background, the 5σ threshold is more suitable at higher dissolved background levels as less background signals may be mistaken for NP intensities (Tuoriniemi *et al.*, 2012; Navratilova *et al.*, 2015).

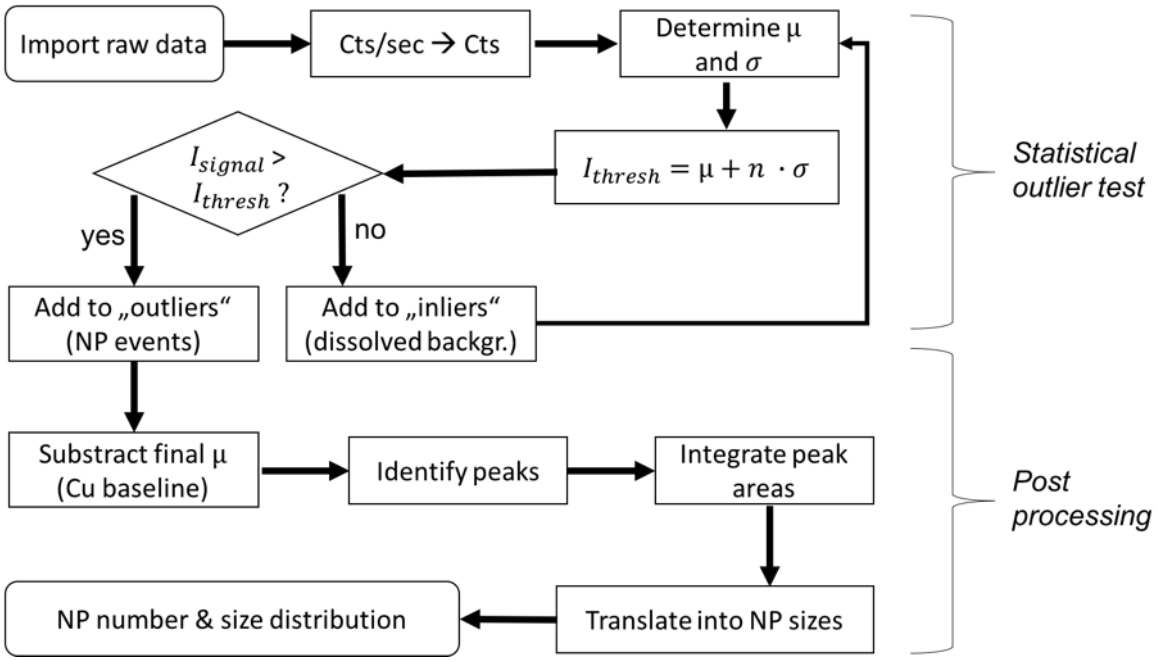

Figure 6: Flow chart on spICP MS data processing. Imported raw data is reduced via an iterative statistical outlier test that is based on mean μ and standard deviation σ of the measured intensities. Signal intensities I_{signal} that are larger than the threshold intensity I_{thresh} are considered as NP events. Once the dissolved baseline is removed, these signal intensities are translated into NP sizes and a NP number and size distribution of each measurement is obtained.

In the post processing step, the resulting “outlier” data (≈ 0,5 % of raw data) is treated further by removing the dissolved Cu baseline (μ) and by identifying and integrating the NP peak areas. The translation into NP sizes is then performed in three steps:

First, the transport efficiency needs to be determined. The transport efficiency is defined as the difference in mass transport between ions from dissolved solution and ions from single particles in spICP-MS (Pace *et al.*, 2012). It is calculated via standard calibrations

that are performed at the start of the measurement session. In these calibrations dissolved Cu and dissolved Gold (Au) standards of known concentration and Au NPs of known sizes (60, 100, 200 nm) are measured. Linear regression curves (Element mass [fg] vs. signal intensity [cnts]) are then plotted and the slope difference between the dissolved Au and the Au NP lines, presenting the transport efficiency, is than applied to the dissolved Cu line to obtain a theoretical Cu NP line. The slope of this theoretical Cu NP line is then used to translate Cu signal intensities to Cu masses (eq. 3).

$$m_{Cu} = \frac{I}{k} \tag{3}$$

The Cu mass (m_{Cu}) is determined by dividing the signal intensity (I) by the slope (k) of the theoretical Cu NP calibration line.

Second, the chemical composition of the material is assumed. By making use of the material-specific fraction Cu and density, NP mass and volume can be determined, respectively.

$$V_{NP} = \frac{m_{mat}}{\rho_{mat}} = \frac{\frac{m_{Cu}}{f_{Cu}}}{\rho_{material}} \tag{4}$$

Where the NP Volume (V_{NP}) is the quotient of material mass (m_{mat}) to material density (ρ_{mat}). The material mass is a result of the Cu mass (m_{Cu}) which was determined in (equ. 3) and the material-specific Cu fraction (f_{Cu}). Details on the assumed compositions in this study are listed in the Appendix, Table A 1.

Third, the NP diameters are determined by assuming a spherical particle shape:

$$\emptyset = 2 \times R = 2 \times \sqrt[3]{\frac{V_{NP}}{4/3\,\pi}} \tag{5}$$

Where the NP diameter ($\emptyset$) is twice the radius (R) of a hypothetical sphere which equals the cubic root of the NP Volume (V_{NP}) divided by 4/3 times π. The equivalent sphere diameters will be referred to as NP sizes hereafter and reported in [nm].

Once the data processing is completed, the R script saves the NP signal intensities and NP sizes in two separate data files (.csv) and a plot showing the NP size distribution diagram with mean and median size for each sample. This is done for each n σ applied. A graphical summary of the data processing performed in R is given in Figure 7. The R script was applied on all data collected during the spICP-MS measurements.

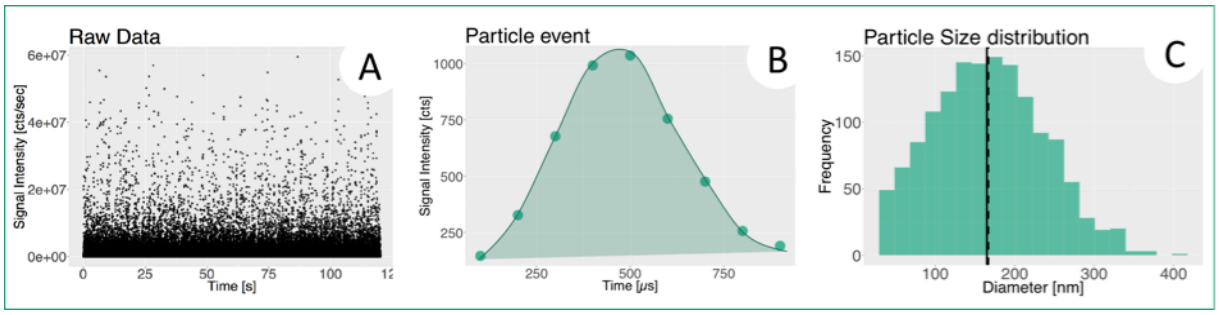

Figure 7: Graphical summary of data processing steps: ***A)*** *Raw data* ***B)*** *isolation and integration of signal pulses* ***C)*** *Conversion of pulse intensities to particle sizes and size distribution. The plane and dashed black lines in this exemplary distribution diagram represent mean and median size, respectively.*

3. Results & Discussion

First, the outcome of the initial characterization of the pristine test materials using spICP-MS is presented (3.1). This is followed by the development of the soil pH over time (3.2) and the findings from the total Cu measurements (3.3), including both i) bioavailable Cu in $CaCl_2$ extracts (3.3.1) and ii) total Cu concentrations in the colloidal extracts (3.3.2). Ultimately, the results from single particle analysis are presented as a series of particle size and number distributions over time.

3.1 Characterization of pristine materials

Throughout this chapter, the results based on the 5σ threshold are presented. This is done to ensure consistency and minimum contribution from the dissolved background signal (Tuoriniemi *et al.*, 2012; Navratilova *et al.*, 2015). In accordance with the number of "particle events" observed in the ionic Cu and blank control, it was assumed that particle frequencies between 0 – 5 in a 60 second measurement represent false positives and a NP content in the respective sample is negligible.

The initial characterization of the test materials reveals detectable NPs in freshly prepared CuO NP and Kocide suspensions. A median particle size of 103 nm is determined for CuO NP and median particle size of 113 nm for Kocide (Figure 8). Yet, the low number of detectable NPs in Kocide suspension does not yield a clear size distribution. Using the 5σ approach, NPs are neither detected in Bordeaux nor in Cupravit samples. As a reference, the

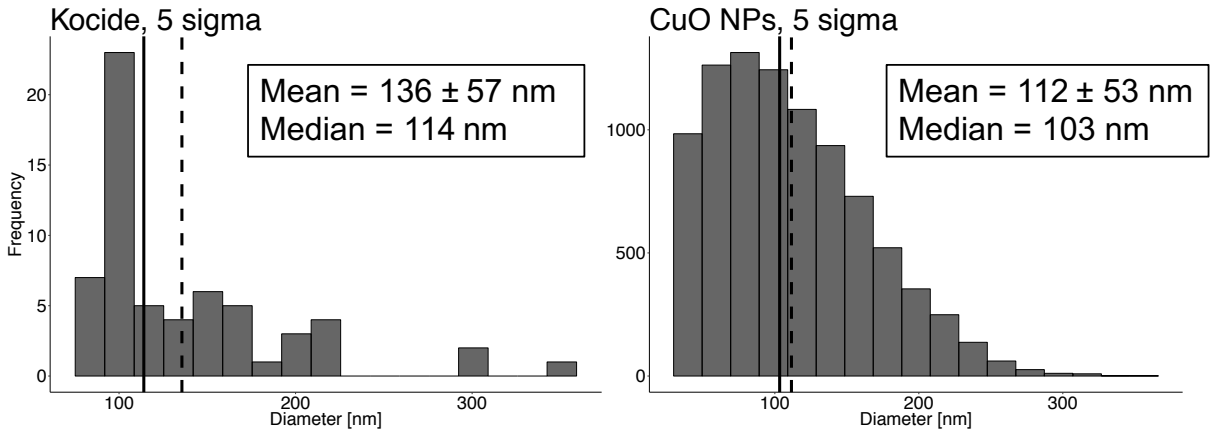

Figure 8: Size distribution diagrams of pristine materials suspended in 1% FL70 matrix. Using the 5σ threshold, NPs were successfully detected in freshly prepared Kocide (left) and CuO NP (right) suspensions.

according size distribution diagrams are presented in Figure A 1 in the appendix. This indicates that the Bordeaux and Cupravit are either entirely dissolved during analysis or contain particles below the size limit of detection (LOD).

Table 2: Results from data processing of pristine materials. Pristine CuO NP suspension contains more detectable NPs than Kocide. The dissolved Cu baseline is ~10 times higher for Kocide relative to CuO NPs. Consequently, the 5σ threshold is higher for Kocide.

Material	Particles/µl^{-1}	Particles/mg material	Baseline [cnts]	Thresh. (5s) [cnts]
Kocide	12	1,1E7	110	365
CuO NPs	1020	1,1E9	10	43

Table 3: Statistics on particle sizes determined in Kocide and CuO NP suspensions. Kocide NPs exhibits larger average NP size and a larger minimum NP size relative to CuO NPs. This may be due to an elevated dissolved Cu background which determines the detection threshold and the size limit of detection.

Material	Mean [nm]	Median [nm]	Std [nm]	Max. size [nm]	Min. size [nm]
Kocide	136	114	57	356	89
CuO NPs	112	103	53	351	34

Regarding the detectable NPs, the dissolved Cu baseline is 10 times higher for Kocide than for the CuO NP measurement indicating a higher fraction of dissolved, ionic Cu. The smallest detected particle sizes are 89 nm and 34 nm for Kocide and CuO NPs suspensions, respectively (Table 2). The difference can be explained by the elevated Cu baseline in the Kocide suspension that affected the threshold (cut-off between the dissolved background and the NP signals) and thereby the size limit of detection (LOD) of this method. The size LOD equals the minimum detectable particle size within a sample. It is therefore very likely that, especially within Kocide, more NPs exist below the size LOD, which were yet not detectable due to an overlapping dissolved and particulate signal (Laborda *et al.*, 2011). Moreover, the average size (Table 3) of CuO NPs is larger in this study than the one provided by the supplier (112-103 > 50 nm). Both median NP sizes in this study occur approximately at 100 nm inferring that ~50% of the material is < 100 nm. This suggests that both CuO NPs and

Kocide may potentially be categorized as NM according to the definition proposed by the EC (European Commission (EC), 2011).

3.2 Soil pH

The pH values measured in the soil $CaCl_2$ extracts range from 5,4 - 6,5. Figure 9 reveals that all treatments follow the same trend: An increase in pH occurs from day 0 to day 4 (pH = 6,1 ± 0,1 to pH = 6,4 ± 0,01; n = 6) after soil amendment. A steady decrease follows until day 21 (pH = 6,4 ± 0,01 to pH = 5,6 ± 0,1; n = 6). Details on the pH values of each soil treatment and incubation day are given in Table 4. Under consideration of the standard deviations, all soil treatments exhibit comparable pH values on each measuring day.

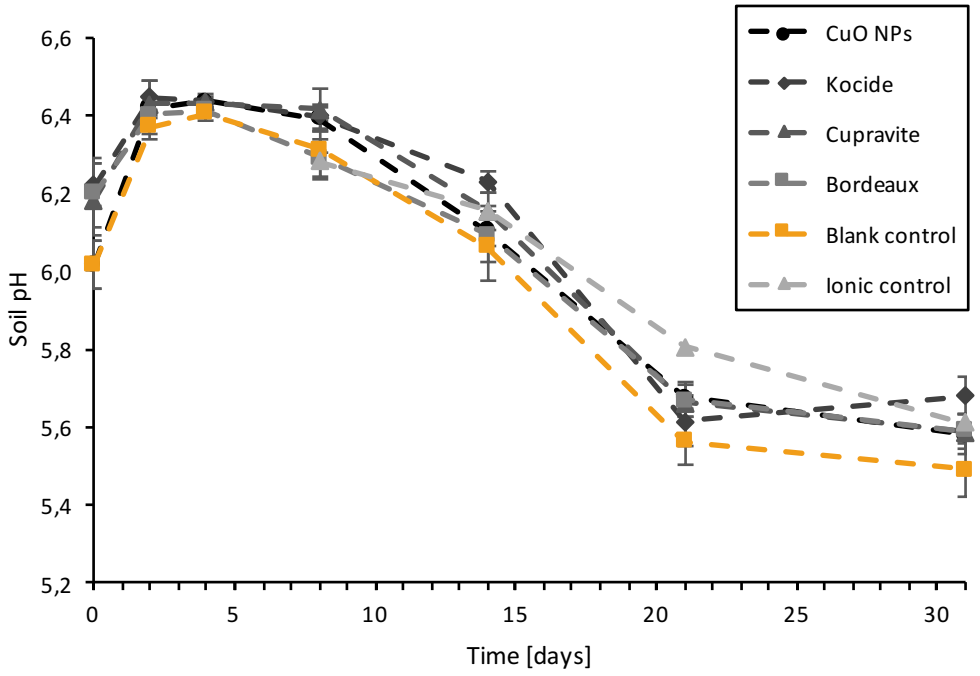

Figure 9: Soil pH over time. The pH values of all soil treatments, including the blank control (orange), follow the same trend of a sharp increase within the first two days, followed by a steady decrease until day 21. The final pH corresponds to the one provided for LUFA 2.2 standard soil and indicates equilibrium conditions by the end of the study period.

Since this trend includes the blank control incubation, it can be stated that pH changes occur independent from the added Cu compounds. They rather reflect the equilibration of the initially dry soil with the added water. The pH reported for LUFA 2.2 standard soil (pH = 5,4 ± 0,2) supports this, as it is approached by the end of the study (5,6 ± 0,1) (Landwirtschaftliche Untersuchungs- und Forschungsanstalt, 2015).

Table 4: Development of soil pH of the individual treatments. Values present the mean pH (n = 3) with standard deviation (Std) measured in the $CaCl_2$ extracts and are comparably for all treatments on each measuring day. Note that pH values were not determined for the ionic Cu control on days 0-4 (N.A.).

Day	**Blank control**		**Ionic control**		**Bordeaux**		**Cupravite**		**Kocide**		**CuO NPs**		**All**	
	Mean	*Std*	*Mean*	*Std*	*Mean*	*Std*	*Mean*	*Std*	*Mean*	*Std*	*Mean*	*Std*	*Mean*	*Std*
0	6,0	0,1	N.A.	N.A.	6,2	0,1	6,2	0,1	6,2	0,1	6,0	0,1	6,1	0,1
2	6,4	0,0	N.A.	N.A.	6,4	0,0	6,4	0,0	6,4	0,0	6,4	0,1	6,4	0,0
4	6,4	0,0	N.A.	N.A.	6,4	0,0	6,4	0,0	6,4	0,0	6,4	0,0	6,4	0,0
8	6,3	0,1	6,3	0,0	6,3	0,0	6,4	0,1	6,4	0,0	6,4	0,0	6,4	0,1
14	6,1	0,1	6,2	0,1	6,1	0,1	6,2	0,1	6,2	0,0	6,1	0,0	6,1	0,1
21	5,6	0,1	5,8	0,0	5,7	0,0	5,7	0,0	5,6	0,1	5,7	0,0	5,6	0,0
31	5,5	0,1	5,6	0,0	5,6	0,0	5,6	0,0	5,7	0,0	5,6	0,0	5,6	0,1

Processes that may govern these pH changes are likely reversed processes from drying and include: the dissolution of precipitated salts, hydrolysis of metals, the dissolution of coagulated dissolved organic matter (DOM), the (de)protonation of organic acids and the reactivation or resting microorganisms. The latter may cause CO_2 release due to microbial respiration. Hence, all of these processes can cause soil pH changes like the ones that were observed during this study (Carter and Gregorich, 2006; Sposito, 2008; Tan, 2010). Consequently, it is likely that the relatively high organic carbon (OC) content of LUFA 2.2 standard soil (OC = 1,61 ± 0,15 %) plays a vital role in these pH changes: First, because mineral phases are more resistant to drying (Carter and Gregorich, 2006) and second, as Gao et., 2017 reported a stable soil pH in a similar study conducted with LUFA 2.1, a standard soil with a lower OC content (OC = 0,71 ± 0,08) (Landwirtschaftliche Untersuchungs- und Forschungsanstalt, 2015; Gao *et al.*, 2017).

Thus, to avoid pH changes, sufficient pretreatment of LUFA 2.2 standard soil is suggested for future studies using this very soil. A stable pH is crucial since it strongly affects ion availability in soil (Sposito, 2008; Tan, 2010). The respective observations of Cu availability are subject of the following chapter.

3.3 Total Cu

3.3.1 Bioavailable Cu ($CaCl_2$ extracts)

The trend of bioavailable Cu extracted over time will be first presented for the control settings and then for the PPPs and CuO NPs incubated soil. Table A 2 gives a summary of the measured Cu concentrations.

In the control treatments, the bioavailable Cu concentrations range from 0,43 ± 0,02 to 1,77 ± 0,05 mg kg^{-1} dry soil in the ionic control and from 0,01 to 0,02 mg kg^{-1} in the blank control. Hence, Cu bioavailability is 30 - 70 times greater in the soil dosed with the ionic control than in the blank control. Considering the Cu bioavailability over time, Figure 10 shows that bioavailable Cu decreases rapidly within the first 8 days: In the ionic and in the blank control by 75 % (from 1,77 ± 0,05 to 0,43 ± 0,02 mg kg^{-1}) and 65 % (0,02 ± 0,00 to 0,01 ± 0,00 mg kg^{-1}), respectively. In the ionic control, an increase of 45 % (from 0,43 ± 0,02 to 0,78 mg kg^{-1}) is observed from days 8-31. Hence, Cu concentrations are highest at the start and show an increase towards the end of the study.

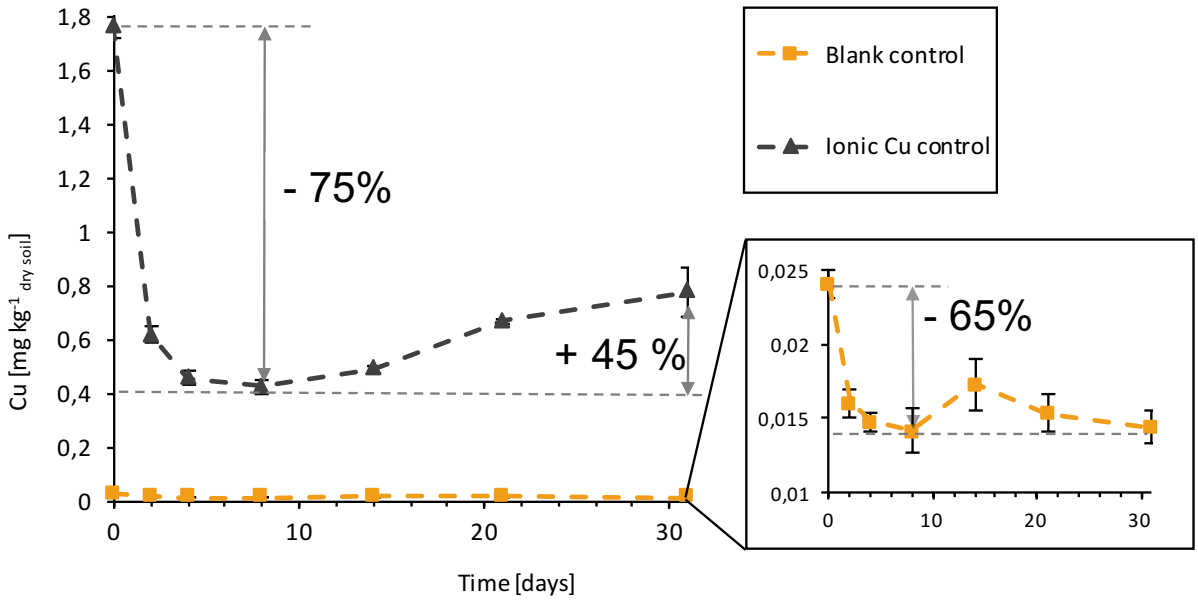

Figure 10: Control settings: Bioavailable Cu [mg kg^{-1} dry soil] extracted from ionic (black) and blank (orange) control soil incubations. An initial decrease of 75-65 % is observed in both treatments within 8 days after dosing. The amount of extracted Cu then increases in the ionic control by 45% until the end of the study.

Bioavailable Cu concentrations of the PPP dosed soils range from 0,42 ± 0,01 to 1,31 ± 0,03 mg kg^{-1}, thus 40 to 65 times above the natural background measured in the blank control. Figure 11 reveals a sharp initial decrease in bioavailable Cu within the first 8 days: in

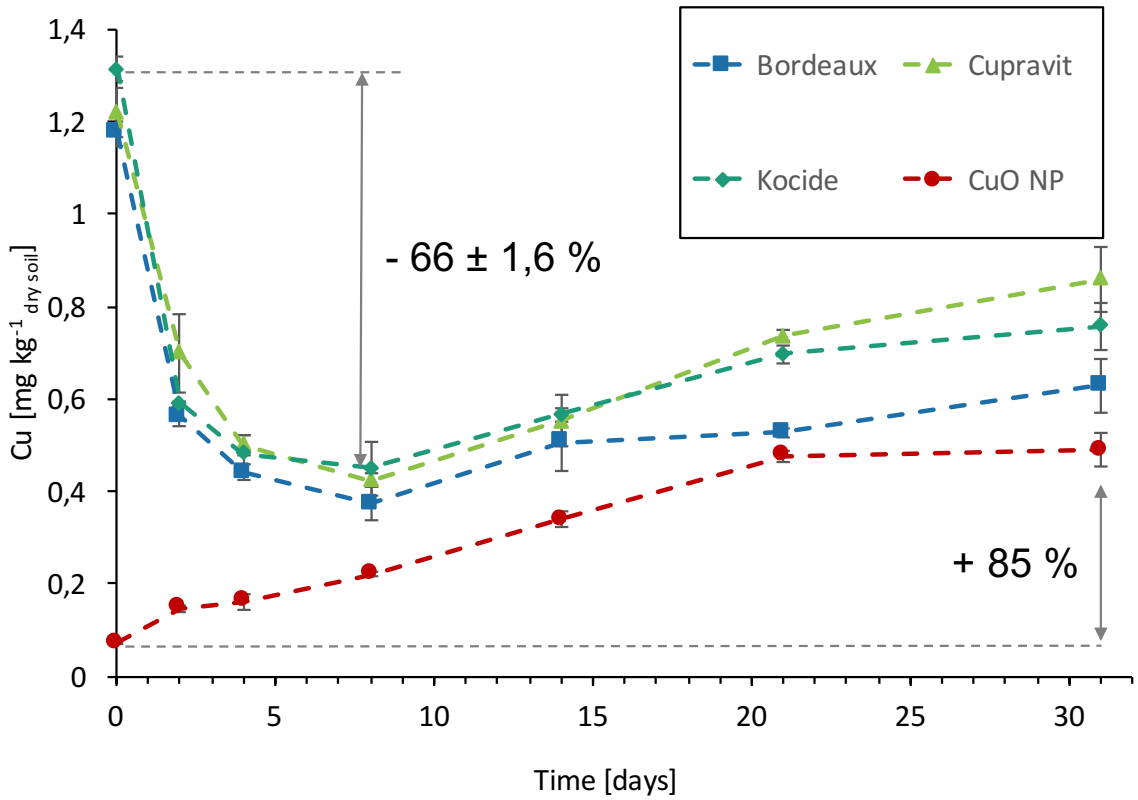

Figure 11: PPP (Bordeaux, Cupravit, Kocide) and CuO NP dosed soil: Bioavailable Cu over time. Whereas the PPP dosed soils show an overall decrease, CuO NP dosed soil shows an increase by 85 % in bioavailable Cu over time. The PPP trend is characterized by an initial Cu decrease of ~66 ± 1,6 % (n =3) and a steady increase of ~44 ± 5,6 % (not specifically highlighted in the graph) after day 8. Most likely a decreasing soil pH enhances Cu lability at this stage.

Bordeaux by 68 % (from 1,17 ± 0,02 to 0,37 ± 0,03 mg kg^{-1}), in Cupravit by 65% (from 1,22 ± 0,05 to 0,42 ± 0,01 mg kg^{-1}) and in Kocide by 66 % (from 1,31 ± 0,03 to 0,45 ± 0,06 mg kg^{-1}). Subsequently, a steady Cu increase is observed from day 8 to the end of the study: in Bordeaux by 41 % (to 0,63 ± 0,06 mg kg^{-1}), in Cupravit by 51 % (to 0,86 ± 0,07 mg kg^{-1}) and in Kocide by 41 % (to 0,76 ± 0,05 mg kg^{-1}). Hence, all soils dosed with Cu based PPPs show a declining Cu bioavailability with time and, thus, exhibit the same trend as observed in the ionic and blank control.

Regarding the soil treated with CuO NPs, the concentration of bioavailable Cu ranges from 0,07 ± 0,00 to 0,49 ± 0,04 mg kg^{-1}. Ionic Cu from CuO NP is thus 10 - 24 times above the natural background of the blank control. Yet, contrary to the previously discussed trend, this soil treatment exhibits initially lower Cu concentrations that steadily increase over time. By the end of the study, an increase of 85% in Cu concentration is observed (Figure 11).

Thus, two principle trends describe Cu bioavailability over time in this study: One trend that shows a rapid decrease in bioavailable Cu at the start and an increase towards the

end of the study and another trend that shows a steady increase of bioavailable Cu with time. The first trend has been observed in the soils dosed with Bordeaux, Cupravit, Kocide and the control solutions likely due to the prevalence of dissolved Cu in these materials and its strong sorption affinity to SOM (Mengel *et al.*, 2001). In contrast, an increase in the Cu bioavailability over time was observed for the soil dosed with CuO NPs. Both observations are consistent with the findings from Gao et al., 2017 and McShane et al., 2014. These studies identified a decrease in the bioavailable Cu concentration with time in soils amended with Cu salt, whereas an increased ionic Cu concentration with time was reported for soils amended with CuO NPs (McShane *et al.*, 2014; Gao *et al.*, 2017).

Regarding the trend observed in the soils dosed with the conventional PPP and the controls, a discrepancy occurs between the findings of Gao et al. (2017) and this study: The authors do not report a secondary increase in Cu availability towards the end of the soil incubation. However, this can be explained by the usage of a different standard soil (LUFA 2.1) that was not prone to soil pH changes (Gao *et al.*, 2017). The increase observed in bioavailable Cu from days 8-31 in the soils from this study, can be attributed to the decrease in soil pH, which occurred over the same period (Figure 9) (Mengel *et al.*, 2001; Sposito, 2008; Tan, 2010). The depletion of total Cu in the bioavailable soil fraction is observed in all soil treatments, except for CuO NP dosed soil. Ma et al. (2006) and Lu et al. (2009) observed increasing complexation of ionic Cu by SOM with time and micropore diffusion that may explain this decline in bioavailable Cu.

The second trend exhibits an increasing Cu bioavailability with time and occurs in soils treated with CuO NPs (McShane *et al.*, 2014; Gao *et al.*, 2017). As shown by Gao et al., bioavailable Cu becomes more extractable with time due to the dissolution of CuO NPs in soil. The dissolution rate is identified as the restricting factor in ionic Cu release (Gao *et al.*, 2017).

3.3.2 Total colloidal Cu

Besides the fraction of bioavailable Cu, the colloidal bound Cu was investigated in this project to assess Cu partitioning from PPP and CuO NP sources. This was achieved by sequential colloidal extractions. The exact concentrations are listed in the Appendix in Table A 3 and illustrated as a sequence of bar charts in Figure A 2. To summarize the Cu proportions, it can be stated that the amount of Cu decreases with extraction number: The first, the second and the third extracts contain in average 39,8 ± 4,7 %, 32,3 ± 3,6 % and 27,9 ± 4 % (n = 147) of the total extracted Cu, respectively.

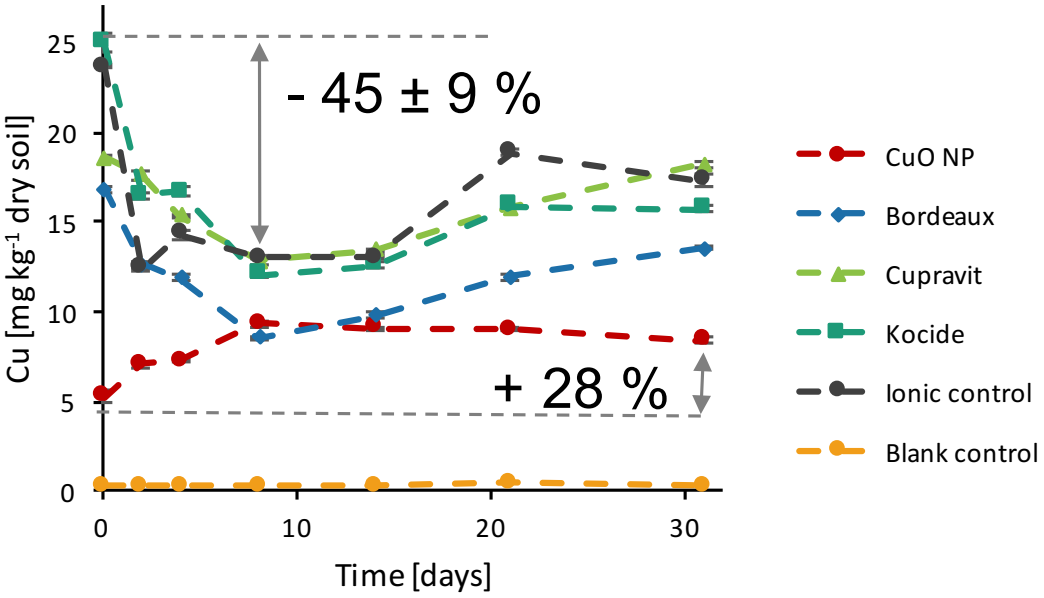

Figure 12: Total Cu in colloidal extracts (summed 1 to 3). Error bars are within the symbol size. PPPs (Bordeaux, Cupravit, Kocide) and ionic control show an instant decrease in colloidal Cu of ~45 ± 9 % within the first 8 days. CuO NPs show a steady increase of 28 %.

Figure 12 shows the total Cu concentrations in the colloidal extracts (summed values for extracts 1-3) over time. The Cu level of the ionic control is > 50 times elevated above the natural background concentration of the blank control: Ionic control Cu levels range from 12,97 ± 0,09 to 23,66 ± 0,11 mg kg^{-1} and the blank control Cu levels from 0,24 ± 0,00 to 0,41 ± 0,01 mg kg^{-1} in the colloidal extracts. The ionic control exhibits the same trend as in the bioavailable Cu extracts: A decrease in total Cu over time until day 8 followed by an increase until the end of the study. The blank control does not show a clear trend under considering of the standard deviations (std).

The PPP treatments exhibit total Cu in the colloidal extracts that is elevated by 30 – 90 times above the natural background of the blank control. Bordeaux has the smallest Cu levels among the PPPs in the colloidal extracts ranging from 8,56 ± 0,11 to 16, 8 ± 0,17 mg kg^{-1} with minimum Cu levels on day 8, a decrease of 49 %. Yet, an increase is then observed by 37% until day 31 (13,54 ± 0,11). Cu levels in Cupravit colloidal extracts range from 12,84 ± 0,2 to 18,55 ± 0,14 mg kg^{-1} with a minimum level on day 8. An increase of 29% follows until day 31 (18,2 ± 0,15 mg kg^{-1}). Kocide derived Cu levels range from 12,03 ± 0,1 mg kg^{-1} to 24,98 ± 0,47 mg kg^{-1} and equally exhibit a minimum level on day 8. A steady increase of 23 % is then observed until day 31 (15,69 ± 0,18). Thus, all PPPs follow the same trend of decreasing Cu levels in the colloidal extracts with time. The levels decline until day 8 before steadily increasing until the end of the study. However, the final levels remain below the maximum Cu concentrations determined on day 0; thereby matching the observations from the $CaCl_2$ extracts (3.3.1).

The Cu concentrations in the colloidal extracts of CuO NP dosed soil are 20 to 70 times above the natural background and range from 5,26 ± 0,32 to 9,34 ± 0,19 mg kg^{-1}. They exhibit an increase by 28 % until day 31 (8,41 ± 0,14 mg kg^{-1}). However, a maximum concentration is determined on day 8 (9,34 ± 0,19 mg kg^{-1}). Besides this elevation, the CuO NP dosed soil exhibits a trend in total Cu in the colloidal extracts that is similar to the one observed in the bioavailable Cu extracts.

The colloidal soil fractions of the ionic Cu control, Bordeaux, Cupravit and Kocide treatments, total Cu concentrations are highest at the beginning of the study. The concentrations then decrease rapidly until day 8 before increasing again. This trend is comparable to the one observed for these materials in the bioavailable Cu fraction. Yet, in the colloidal soil fraction, the measured concentrations are greater (1-2 orders of magnitude) and the relative differences over the period smaller. This trend may be explained by increasing SOM complexation with time as suggested by Ma et al. 2006, and Lu et al., 2009 (Ma *et al.*, 2006; Lu *et al.*, 2009). A larger amount of these Cu complexes may be present in the colloidal extracts, thus, yielding the higher total Cu concentrations in comparison to the bioavailable Cu extracts. Nevertheless, ionic Cu and potentially complexed Cu also deplete with time from the colloidal soil fraction. The excess Cu is likely to be associated with the soil fraction removed during centrifugal separation. However, a

secondary increase in total Cu concentration in the colloidal extracts is observed towards the end of the study. This is likely due to a simultaneous decline in soil pH that remobilizes ionic Cu (Tan, 2010).

In the colloidal soil fraction of CuO NP dosed soil, a steady total Cu increase is observed with time, yet at higher Cu concentrations than in the bioavailable soil fraction. Again, the increasing Cu trend can be attributed to ionic Cu release with increasing incubation time by NP dissolution, as shown by Gao et al. (2017). However, since this trend occurs in the extracts that were aimed to contain NPs and soil colloids, it can be assumed that the ionic Cu sources, namely the CuO NPs, are partially associated with the soil fraction removed by centrifugation. This may have been caused by particle (hereto)aggregation and subsequent sedimentation.

In summary, the total Cu concentrations in both extraction types followed one of two trends: Whereas total Cu in the ionic control and the PPP dosed soils showed a decrease over the first 8 days of incubation and a subsequent increase with time, Cu from CuO NPs increased steadily until the end of the experiment. Moreover, the soil pH appeared to play a key role in Cu partitioning. Higher Cu concentrations were determined in the colloidal extracts relative to the bioavailable ones (1-2 orders of magnitude). In the colloidal soil fraction, Cu is likely present either as NP or in form of SOM complexes and/or sorbed to soil colloid surfaces (Tan, 2010).

3.4 Nanoparticle Characterization

spICP-MS analysis revealed detectable NPs in the colloidal extracts from two of the soil treatments. The presented data is the result of the statistical outlier test performed with a 5σ cut-off. In accordance with the number of "particles" observed in the ionic and blank Cu control, it was assumed that particle numbers between 0 – 5 in a 60 second measurement represent false positives and a NP content in the respective sample is negligible.

3.4.1 Detectable CuO NPs

CuO NPs were successfully extracted from soil using the sample preparation protocol outlined in section 2.5 and detected with spICP-MS. Figure 13 shows a compilation of obtained particle size distribution diagrams for each sampling and measuring day (0, 2, 4, 8,

14, 21 and 31). Each histogram (NP frequency vs. size [nm]) presents a combined view of all three sequential colloidal extracts measured for 60 seconds each. Full details on the particle sizes and standard deviations of the individual extracts are reported in Table A 10 in the Appendix.

On day 0, the computed NP sizes range from 30 to 565 nm. The mean NP size is 106 ± 61

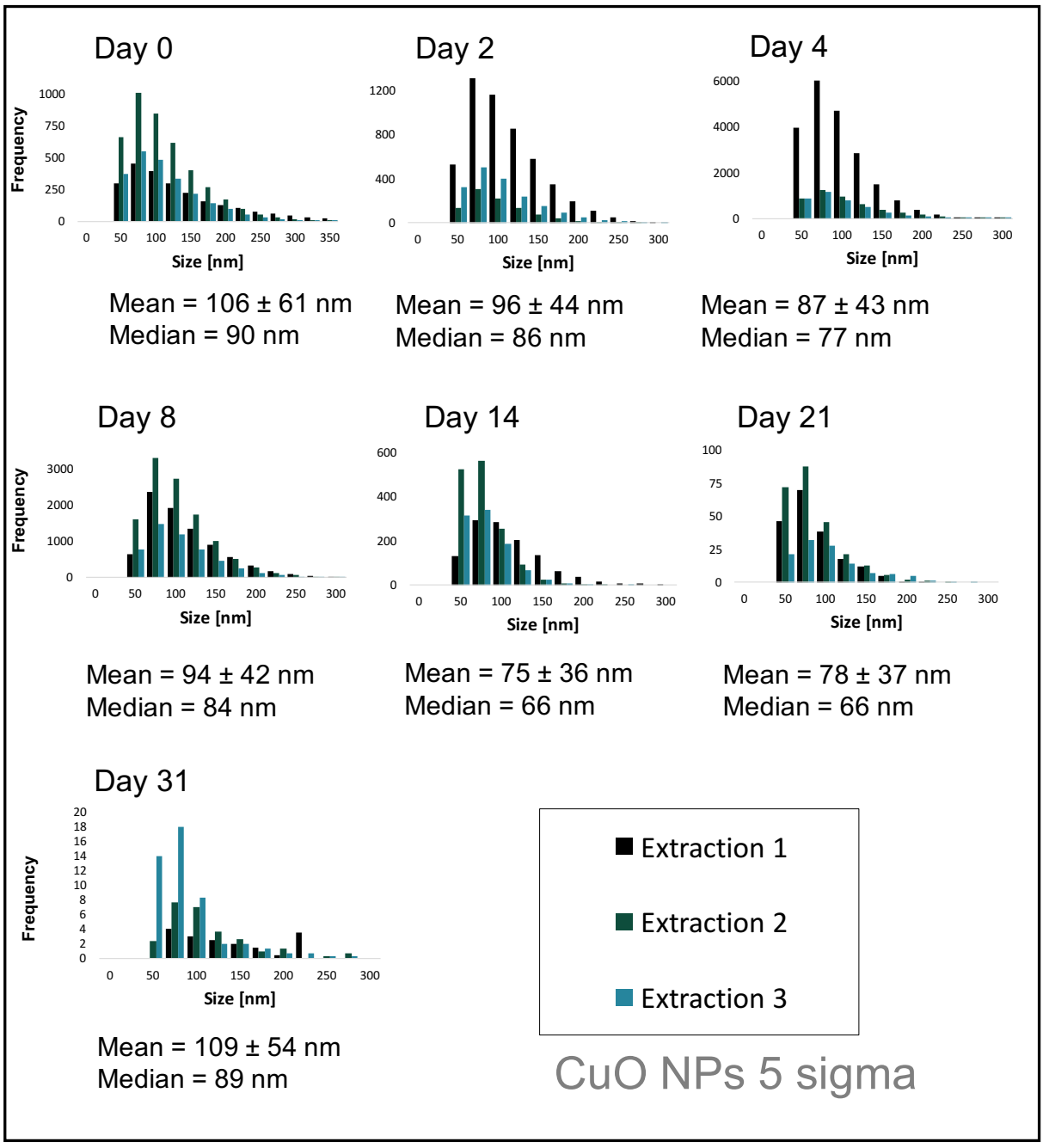

Figure 13: CuO NP size distribution diagrams with time. The individual diagrams show a compilation of NP size distribution diagrams (NP size [nm] vs. frequency) from NPs detected in extracts 1, 2 and 3. Average sizes in the graph cover extracts 1 to 3 and generally decrease with time. Exceptions are days 8 and 31. The diagrams generally shift to smaller sizes over time. The frequencies decrease notably after day 4.

nm (all three extracts combined). This value is comparable to the average particle size of the pristine material (112 ± 53 nm). In the colloidal extracts, the mean NP size decreases to 87 ± 43 nm until day 4 where the minimum and the maximum particle sizes are 34 and 377 nm, respectively. Thus, a decrease in NP size and size range is observed within the first four days. Nevertheless, the shift in NP frequency (y-Axis) reveals a sharp increase in the particle number until day 4. On day 8, NP sizes range from 40 to 355 nm with a mean size of 94 ± 42 nm. The mean size decreases to 78 ± 37 nm until day 21, where sizes range from 37 to 378 nm. Hence, a clear decrease in NP size is observed following day 8. Yet, on day 31, a mean size of 109 ± 54 nm is determined within range of 47 to 309 nm. The NP frequency decreases steadily from day 8 to day 31.

Thus, Figure 13 reveals a general decrease in NP size over time, with two exceptions: On day 8 and 31, average NP sizes are larger than on the preceding time points. Nevertheless, this can be explained by equally higher size LODs on the respective measuring days. As previously explained, an elevated size LOD is the result of a high dissolved Cu background whose signal partially overlaps with NP signals (Laborda *et al.*, 2011). The computed sizes are consequently biased towards larger sizes; thereby affecting the computed mean NP size of the sample. This explanation is supported by the observations from total Cu measurements in the colloidal extracts as comparably high total Cu concentrations are determined on days 8 and 31 (Figure 12). In addition, the low particle number on day 31 reduced the quality of the statistics. Thus, it can be stated that despite the computation of larger mean sizes on days 8 and 31, NP sizes generally decrease with time in the colloidal extracts from CuO NP dosed soil. A shift towards smaller particle sizes in the diagrams and an increasingly narrow NP size range support this observation.

Regarding the NP frequencies, an initial increase in detectable NPs can be observed until day 4 and a steady decrease until day 31. The quantification of the exact NP number concentrations is shown in Table 5. It reveals an increase from 588 to 1322 particles μl^{-1} colloid suspension from day 0 to day 4 and a steady decrease to 6 particles μl^{-1}.

Resolving the particle number concentrations of the individual extracts reveals on day 0 a maximum particle content in extract 2. On the consecutive days 2 and 4, extract 1 is expected to represent the most loosely bound colloidal fraction in soil and yields the highest particle number concentrations. From day 8 to day 21, extract 2 contains the maximum

number of detectable NPs. On day 31, the maximum number is contained in extract 3 which is expected to represent the most strongly bound colloidal soil fraction. However, the relatively low number of detected particles has likely affected the quality of the statistics on day 31. The trends in particle number concentration are additionally illustrated by Figure 14.

Table 5: Particle number concentration of CuO NP colloidal extract in detectable particles per µl. The maximum number of particles is detected on day 4. Subsequently the number of detectable particles decreases until day 31.

Day	Extraction 1 [particles μl^{-1}]	Extraction 2 [particles μl^{-1}]	Extraction 3 [particles μl^{-1}]	Average Extraction 1-3 [particles μl^{-1}]
0	465 ± 190	834 ± 67	463 ± 40	588
2	1042 ± 84	190 ± 53	363 ± 19	517
4	4084 ± 155	950 ± 180	773 ± 13	1322
8	837 ± 198	1132 ± 342	516 ± 15	828
14	235 ± 49	293 ± 13	188 ± 17	239
21	38 ± 4	50 ± 2	23 ± 4	24
31	4 ± 1	5 ± 0	10 ± 3	6

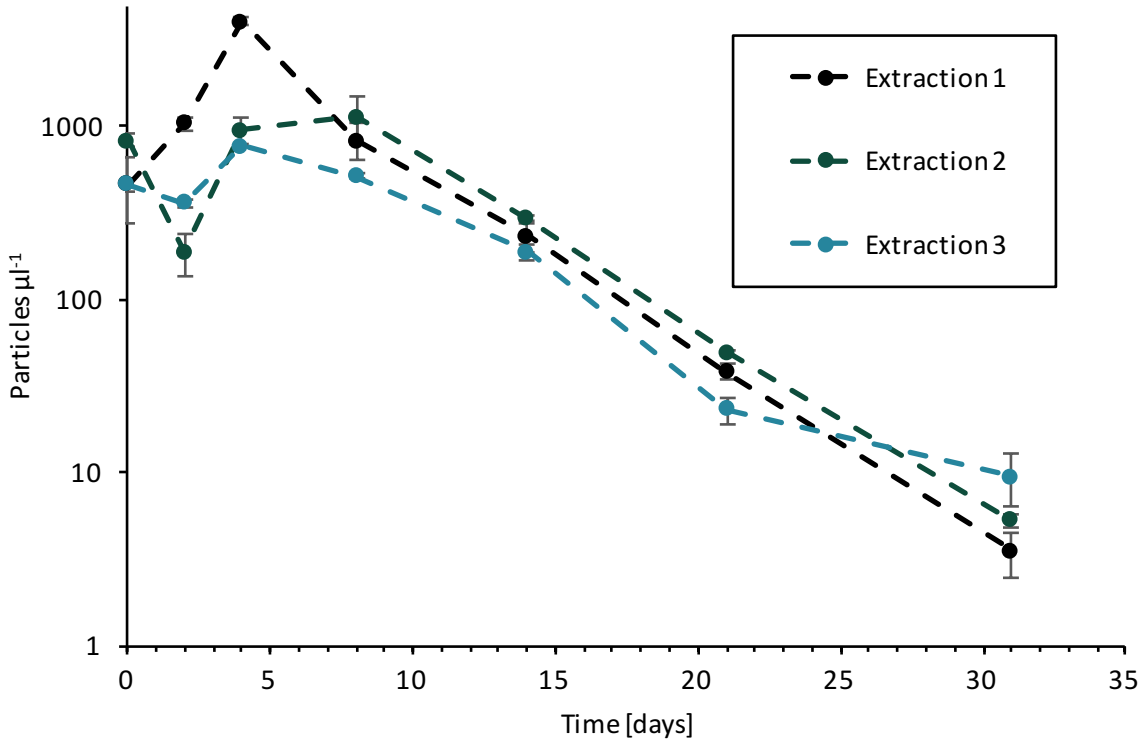

Figure 14: Particle number concentration [Particles µl-1 colloidal extract] with increasing incubation time [days]. Note the semi-log nature of this plot. The number of detectable CuO NPs increases within the first 4 days, before it decreases notably until day 31.

Hence, two main trends can be observed in this data: First, NPs become increasingly detectable within all extracts within the first four days. Yet, this occurs most notably in the first extract which presents the most loosely bound colloid fraction. Second, a decrease of detectable NPs is observed from day 4 on within all soil extracts.

The initial increasing detectability of NPs likely reflects an increasing extractability of NPs. In the same time span (days 0 - 4) an increasing total Cu concentration was observed likewise (Figure 12). This suggests that especially in the beginning of the study, CuO NPs are partially associated with the soil fraction removed by centrifugation. However, CuO NPs reach a maximum extractability on day 4 which may be related to the soil pH. Due to its influence on NP surface charge, increased mobility is often associated with a relatively high soil pH (Cornelis *et al.*, 2014). As the soil pH in this study reaches its maximum value (pH = 6,4 ± 0,1) on day 4, it might have contributed to NP mobilization and thereby NP extractability. However, this was not verified in this study.

The second trend is a decrease in detectable NP number from day 4 to day 31. As this appears simultaneously to an increasing ionic Cu concentration, this trend reflects most likely the dissolution of CuO NPs in soil. This is in accordance with the findings from (Gao *et al.*, 2017), who attributed the increase in ionic Cu in LUFA 2.1 standard soil to CuO NP dissolution. However, NPs were successfully detected until day 31 in this incubation study. Hence, CuO NPs persist in LUFA 2.2 standard soil > 31 days.

Thus far, this study has shown that CuO NPs were successfully detected in colloidal soil extracts from LUFA 2.2 standard soil. This was achieved throughout the study period of 31 days, whereas the number of detectable particles decreased notably after day 4. The mean NP sizes decreased with time as the NP size distribution diagrams shifted towards smaller particle sizes. Under consideration of the results from the previous sections, namely an increasing total Cu concentration over time, the decreasing number and average sizes of detectable NPs are most likely caused by CuO NP dissolution in soil.

3.4.2 Detectable NPs in Kocide

Throughout the study, Cu based NPs were detected in the colloidal extracts from soil dosed with the commercially available PPP Kocide. Figure 15 shows the respective particle size distribution diagrams for the sampling and measuring days (0, 2, 4, 8, 14, 21 and 31). On day 0, the particle sizes range from 84 to 450 nm with a mean size of 143 ± 44 nm. This size is comparable to the mean determined in the initial characterization of pristine Kocide suspension (mean size = 136 ± 57) which verifies the applicability of this method. Regarding

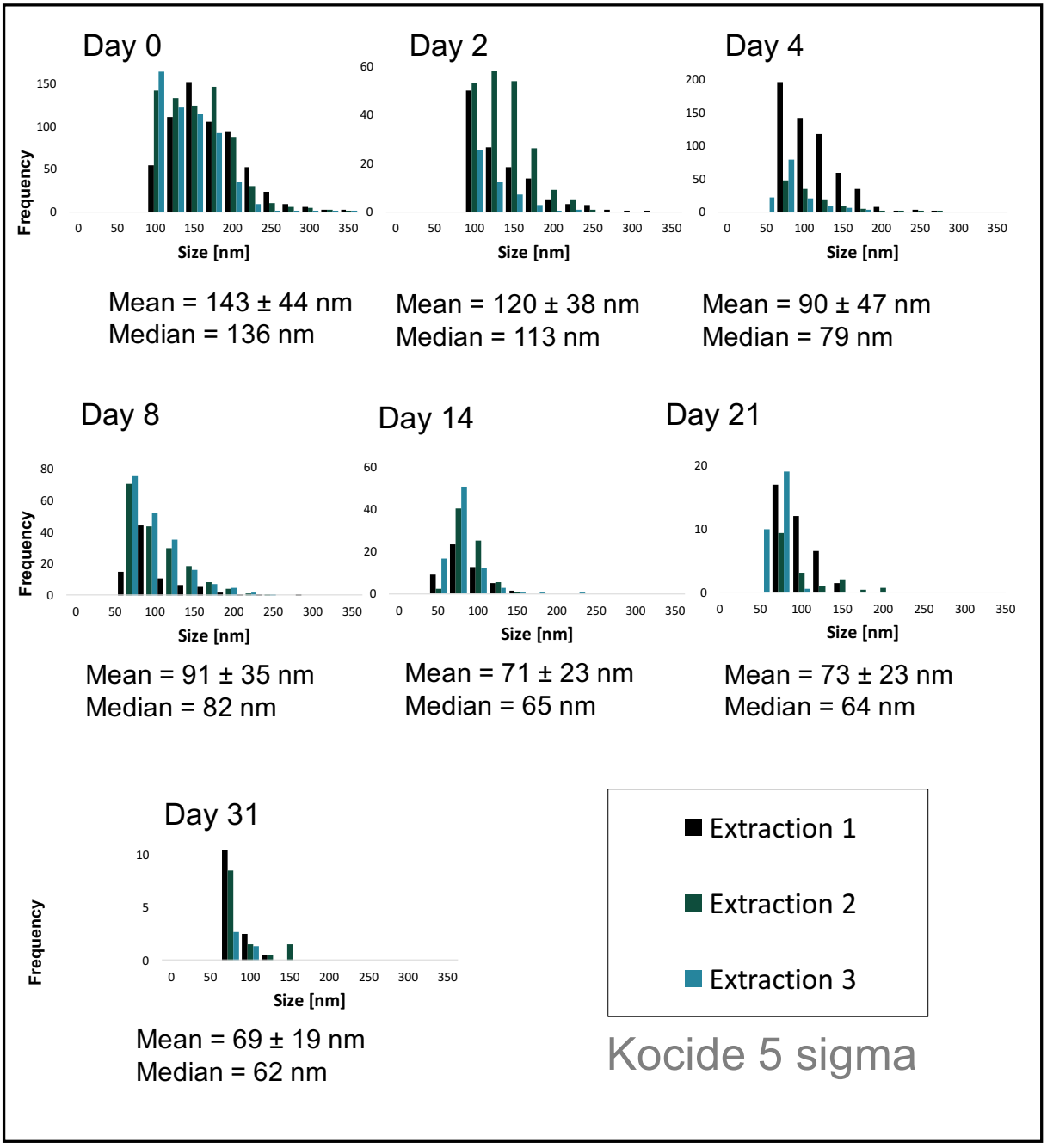

Figure 15: Kocide NP size distribution diagrams with time. The indicated mean and median values cover all three extract and the distribution diagrams show a clear shift towards smaller particle sizes and frequencies with time.

the colloidal extracts, the sizes decrease until day 4 where a mean size of 90 ± 47 nm is determined within a size range of 48 to 270 nm. On day 8, the mean size is 91 ± 35 nm and the minimum and the maximum detectable sizes are 53 and 200 nm, respectively. These sizes decrease to a mean of 69 ± 19 nm on day 31 within a size range of 55 to 146 nm. Full details on the statistics of the computed particle sizes detected in Kocide colloidal suspensions are listed in Table A 11 in the Appendix.

The highest size LOD was determined on day 0 (minimum size = 84 nm). This is in accordance with the dissolved Cu levels which likewise had their maximum on day 0 (Figure 11 and Figure 12). Furthermore, the it can be assumed that the relatively high size LOD has biased the detectable NP towards larger sizes on that day.

Subsequently, the size distribution diagrams show a clear shift towards smaller particle sizes with time. Moreover, the NP size ranges and standard deviations become increasingly smaller. The particle frequencies generally decrease with time, except for day 4. Hence, the trends observed in the particle size distribution diagrams from Kocide are similar to those from CuO NP: The detectable NPs transform to smaller sizes over time, which can be explained by particle dissolution.

Table 6: Particle number concentration in Kocide colloidal extracts. Values present detectable particles per µl colloidal extract. The maximum number of particles is detected on day 4, this is particularly pronounced in extraction 1. Subsequently the number of detectable particles decreases until day 31.

Day	Extraction 1 [particles μl^{-1}]	Extraction 2 [particles μl^{-1}]	Extraction 3 [particles μl^{-1}]	Average Extraction 1-3 [particles μl^{-1}]
0	122 ± 9	137 ± 9	108 ± 7	123 ± 9
2	27 ± 9	14 ± 6	10 ± 6	16 ± 8
4	112 ± 7	24 ± 5	19 ± 5	34 ± 9
8	18 ± 7	13 ± 6	8 ± 6	13 ± 7
14	10 ± 5	10 ± 4	17 ± 4	12 ± 5
21	5 ± 4	4 ± 2	4 ± 2	4 ± 5
31	3 ± 2	2 ± 2	1 ± 2	2 ± 4

The particle number concentrations are shown in Table 6 and reveal that fewer particles (1 order of magnitude) were detected in the Kocide extracts in comparison to the CuO NP samples. This might in part be due to the higher Cu background in Kocide samples which

impedes NP quantification below the size LOD. However, the NP number concentration clearly decreases over time within the extracts from 123 ± 9 to 2 ± 4 particles μl^{-1}.

Regarding the individual extracts, the trends in Figure 16 appear similar, yet, less systematic than those observed in the CuO NP extracts. The particle number concentration generally decreases with time. However, on day 4 it is comparably high, especially in the first extract. Thus, an increase in detectable NPs is observed, particularly in the most loosely bound colloid fraction. This might be due to the relatively low dissolved Cu concentration and low size LOD (48 nm) on day 4 that improve NP quantification. Alternatively, particles may be contained in the extracts that were not extractable on day 2. This may be caused by particle aggregation that hindered extractability on days 0 and 2. Beginning NP dissolution might have decreased then the aggregate sizes < 500 nm. As previously discussed, theoretically also a relatively high soil pH may enhance NP mobility and thus extractability in soil (Cornelis *et al.*, 2014). Regarding day 31, the particle number concentrations are close to the detection limit. Especially in extract 3, it can not be excluded that the signals are false positives and that no more NPs are included in this sample.

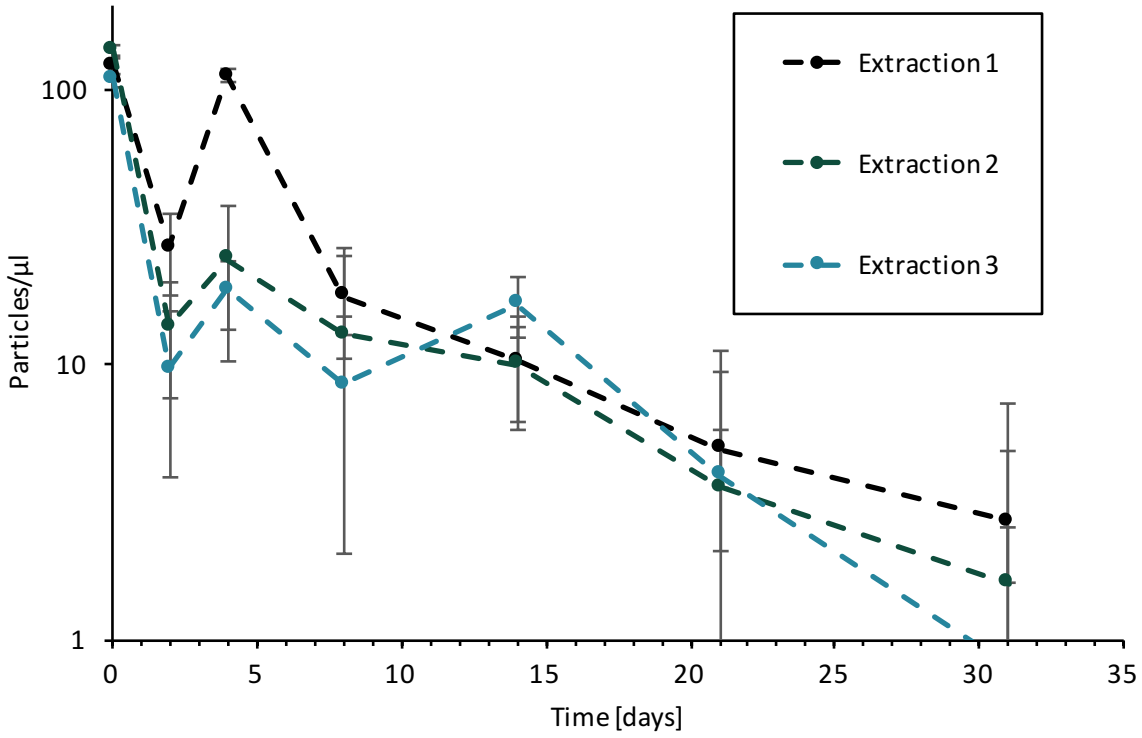

Figure 16: Kocide NP number concentration [Particles µl-1 colloidal extract] with increasing incubation time [days]. Note the semi-log scale of the plot. The number of extracted particles decreases with time in the colloidal soil fraction of Kocide dosed soil.

This section has shown that Cu based NPs were not only present in the soil dosed with CuO NPs, but also in the soil dosed with the commercially available PPP Kocide. Cu based NPs were detected within the colloidal extracts of Kocide throughout the entire study period of 31 days. In general, the Kocide samples exhibit a decrease in particle size and number with time as the particle size distribution diagrams shift towards smaller sizes and frequencies with time. However, on day 31 the Kocide colloidal extracts are characterized by a particle number concentration which is close to the detection limit of the applied method. This is particularly true for extract 3, which appears to be free of particles on day 31.

These observations can be explained by particle dissolution. In contrast to the CuO NPs, however, particle dissolution is not reflected in the results from the total Cu analysis.

3.5 Recap

Total Cu analysis has shown that total bioavailable Cu and total Cu in the colloidal extracts have similar trends. Total Cu increased with time in the soil sample spiked with CuO NPs. This was attributed to ionic Cu release from NP dissolution. In contrast, total Cu decreased with time in the soils dosed with the PPPs (including Kocide) and the ionic control solution. Despite this overall decrease, a minor increase of total Cu was observed in these samples starting on day 8. This was attributed to a decreasing soil pH with time. Such time-dependent pH changes were observed in all soil treatments and stem from an equilibration process between the initially dry soil with the added soil moisture. This was verified by the soil spiked with the blank control solution.

Initial testing of the pristine materials in suspension revealed a high dissolved Cu background for all materials. However, NPs were successfully detected within the suspensions of CuO NPs and one of the PPPs, Kocide. The particle number and size diagrams obtained from the colloidal soil extracts reflect both i) a decrease in detectable NPs and ii) a shift towards smaller sizes with time for CuO NPs and Kocide. Both materials exhibited detectable NPs until the end of the study (day 31). The decline in particle number and size was explained by NP dissolution.

4. Conclusion & Outlook

The aim of this study was to investigate time-dependent transformations of CuO NPs in soil with spICP-MS and to explore potential differences to conventional Cu based PPPs. The results demonstrate the applicability of the presented method and document NP dissolution in soil. Nevertheless, spICP-MS relies on relevant assumptions like NP composition and spherical particle shape. These assumptions can be verified by complementing spICP-MS with other techniques, e.g., SEM or TEM coupled with elemental analysis. The application of SEM was also attempted in this study to confirm spherical particle shapes of the materials and to obtain a second estimate of the NP sizes. Yet, this attempt failed due to difficulties encountered with the sample carrier under high vacuum conditions. Particle characterization by SEM is thus aimed to be repeated under adapted settings.

Besides the assumptions on NP shape and composition, the discrimination between dissolved Cu and NP signals was identified as the main limitation of spICP-MS analysis. Since the size LOD of the presented method depends on the dissolved background concentration, the NP number and average sizes are likewise affected. It is therefore suggested for future studies (aiming to use spICP-MS at high background levels) to apply a different approach, such as signal deconvolution presented by Cornelis and Hassellöv (2014). The R script itself proved to treat the data in a reliable and reproducible manner. The fact that it loops over a list of raw data files and implements the individual measurement names into graphs and file names is very beneficial for the user. The user has the freedom to choose sigma values for the threshold, tailoring the method for specific sample types and dissolved metal backgrounds. Furthermore, the script runs in the open-source software R which can be downloaded for free and for a variety of computer operating systems.

Despite the analytical limitations of the method, NPs are successfully detected using the presented approach. The study concludes that CuO NPs dissolve in LUFA 2.2 standard soil over time. This is reflected by a steady increase of ionic Cu in soil solution and a decrease in detectable particle number and size with time.

In contrast, two conventional PPPs (Bordeaux and Cupravit) and the ionic control exhibit a clearly different behavior. These materials are governed by ionic Cu which depletes rapidly from the bioavailable and the colloidal soil fraction with time. The ionic Cu trends are additionally affected by time-dependent soil pH changes. In future studies, these changes

can be prevented by adequately preconditioning air-dried LUFA 2.2 standard with moisture prior to experiments.

Interestingly, Kocide shows characteristics of both the readily dissolvable PPPs and the CuO NPs. From a total Cu perspective, Kocide shows similar behavior as the two PPPs and the ionic Cu control since bioavailable and colloidal Cu decrease rapidly with time. Yet, this material revealed additionally detectable particles in its pristine state as well as during the soil incubation. The presence of NPs in Kocide is not reflected by total Cu trends obtained from the chemical extraction procedure. This observation highlights that spICP-MS is a more reliable technique for investigating NPs in soil offering a direct mean to detect inorganic engineered NPs in the natural soil matrix.

Contrary to the commercially available PPPs that are known to cause Cu accumulation in soil, CuO NPs may offer the benefit of slow and controlled ionic Cu release with time. Nevertheless, NPs were not fully dissolved until the end of the study indicating a prolonged persistence and ionic Cu release relative to the commercial products. Therefore, assessing the dissolution extent of this material in soils with different characteristic is important. For example, the presented implications do not hold true for soils prone to fluctuating redox conditions, different soil chemistry or a varying degree of soil moisture. Additionally, future studies could assess the dissolution rate and/or the dissolution extent of CuO NPs in soils at elevated Cu background levels. The latter would be a realistic scenario for nano-enhanced PPPs entering agricultural soil with already elevated Cu concentrations from previous PPP applications. The extent of NP dissolution is relevant regarding soil erosion, for example, potentially dispersing NPs from soil into the broader environment.

Nano-enhanced PPPs may not only help reduce Cu application levels and rates in agricultural application, the findings from this and similar studies suggest that CuO NPs exhibit a slower ionic Cu release in soil in contrast to conventional products causing Cu accumulation (Ma *et al.*, 2006; McShane *et al.*, 2014; Gao *et al.*, 2017). Although this presents a potential benefit, the uncertainty of NP persistence in soil and their long-term fate remains. In conclusion, the findings of this study contribute to the understanding of NP transformations in soil and help to inform the safe design of nano-enhanced PPPs. Yet, future studies are needed to unravel the behavior of these materials under varying environmental conditions. This is crucial in order to evaluate whether the usage of nano-enhanced PPPs is a suitable strategy to tackle modern agricultural challenges.

5. References

Agrios, G. (2005) *Plant pathology*. Academic Press. Available at: https://www.elsevier.com/books/plant-pathology/agrios/978-0-08-047378-9.

Baalousha, M., Stolpe, B. and Lead, J. R. (2011) 'Flow field-flow fractionation for the analysis and characterization of natural colloids and manufactured nanoparticles in environmental systems: A critical review', *Journal of Chromatography A*. Elsevier B.V., 1218(27), pp. 4078–4103. doi: 10.1016/j.chroma.2011.04.063.

Barlow, R. J. (1989) *Statistics: A guide to the Use of Statistical Methods in the Physical Sciences*.

Berger, E., Dersch, G., Dellantonio, A., Duboc, O., Manner, K., Möbes-Hansen, B. and Stemmer, M. (2012) 'Kupfer als Pflanzenschutzmittel – Strategie für einen nachhaltigen und umweltschonenden Einsatz', 100537(100537), pp. 1–126. Available at: https://www.dafne.at/prod/dafne_plus_common/attachment_download/5823f55c5b09079fdb5f53763cc1d46a/Abschlussbericht_CuCSM__2012.pdf.

Bundesamt für Ernährungssicherheit, Ö. (2017) *Verzeichnis der in Österreich zugelassenen/genehmigten Pflanzenschutzmittel*, *25.08.2017*. Available at: http://pmg.ages.at/pls/psmlfrz/pmgweb2$.Startup (Accessed: 30 August 2017).

Carter, M. R. and Gregorich, E. G. (eds) (2006) *Soil Sampling and Methods of Analysis*, *Canadian Society of Soil Science*.

Certis USA, L. L. C. (2017) *USER SAFETY RECOMMENDATIONS*. Available at: http://www.certisusa.com/pdf-labels/Kocide3000_label.pdf (Accessed: 29 August 2017).

Cornelis, G. and Hassellöv, M. (2014) 'A signal deconvolution method to discriminate smaller nanoparticles in single particle ICP-MS', *J. Anal. At. Spectrom.*, 29(1), pp. 134–144. doi: 10.1039/C3JA50160D.

Cornelis, G., Hund-Rinke, K., Kuhlbusch, T., van den Brink, N. and Nickel, C. (2014) 'Fate and Bioavailability of Engineered Nanoparticles in Soils: A Review', *Critical Reviews in Environmental Science and Technology*, 44(24), pp. 2720–2764. doi: 10.1080/10643389.2013.829767.

Degueldre, C. and Favarger, P. Y. (2003) 'Colloid analysis by single particle inductively coupled plasma-mass spectroscopy: A feasibility study', *Colloids and Surfaces A: Physicochemical and Engineering Aspects*, 217(1–3), pp. 137–142. doi: 10.1016/S0927-

7757(02)00568-X.

Dubascoux, S., Von Der Kammer, F., Le Hécho, I., Gautier, M. P. and Lespes, G. (2008) 'Optimisation of asymmetrical flow field flow fractionation for environmental nanoparticles separation', *Journal of Chromatography A*, 1206(2), pp. 160–165. doi: 10.1016/j.chroma.2008.07.032.

Elshkaki, A., Graedel, T. E., Ciacci, L. and Reck, B. (2016) 'Copper demand, supply, and associated energy use to 2050', *Global Environmental Change*. Elsevier Ltd, 39, pp. 305–315. doi: 10.1016/j.gloenvcha.2016.06.006.

European Commission (EC) (2002) 'EC No 473/2002', *Official Journal of the European Communities*, (473), pp. 21–24.

European Commission (EC) (2009a) 'Review Report: Copper compounds SANCO/150/08 final 26 May 2009', (1490).

European Commission (EC) (2009b) 'Review report for the active substance Copper compounds Finalised', *HEALTH AND CONSUMERS DIRECTORATE-GENERAL*, 2007(1490), pp. 1–9. doi: 10.2903/j.efsa.2013.3346.

European Commission (EC) (2011) 'COMMISSION RECOMMENDATION on the definition of nanomaterial', (4), pp. 2010–2012.

European Commission (EC) (2013) 'Second regulatory review on nanomaterials.', *Communication from the Commission to the European Parliament, the Council and the European Economic and Social Committee.*, p. Brussels, 3.10.2012, COM(2012) 572 final. doi: 10.1017/CBO9781107415324.004.

European Commission (EC) (2016) *Pesticides - European Commission*. Available at: https://ec.europa.eu/food/plant/pesticides_en (Accessed: 11 October 2017).

European Commission (EC) (2017) *EU Pesticides database - European Commission*. Available at: http://ec.europa.eu/food/plant/pesticides/eu-pesticides-database/public/?event=activesubstance.detail&language=EN&selectedID=1158 (Accessed: 29 August 2017).

Eurostat (2016) *Agriculture, forestry and f ishery statistics 2016 edition*. doi: 10.2785/917017.

Everett, D. (2009) 'Manual of symbols and terminology for physicochemical quantities and units, appendix II: Definitions, terminology and symbols in colloid and surface chemistry', *Pure and Applied Chemistry*, 31(4). doi: 10.1351/pac197231040577.

FAO (1999) *FAO - Position paper on Organic Agriculture*. Rome. Available at: http://www.fao.org/docrep/meeting/X0075e.htm (Accessed: 12 October 2017).

Ford, R. G. and Wilkin, R. T. (2010) 'Monitored Natural Attenuation of Inorganic Contaminants in Ground Water', *Unitedt States Environmental Protection Agency,* 147, p. 147. doi: 10.1680/wama.2008.161.6.381.

Gao, X., Spielman-Sun, E., Rodrigues, S. M., Casman, E. A. and Lowry, G. V. (2017) 'Time and Nanoparticle Concentration Affect the Extractability of Cu from CuO NP-Amended Soil', *Environmental Science and Technology*, 51(4), pp. 2226–2234. doi: 10.1021/acs.est.6b04705.

van Gestel, C. A. M. (2008) 'Physico-chemical and biological parameters determine metal bioavailability in soils', *Science of the Total Environment*. Elsevier B.V., 406(3), pp. 385–395. doi: 10.1016/j.scitotenv.2008.05.050.

Giannousi, K., Avramidis, I. and Dendrinou-Samara, C. (2013) 'Synthesis, characterization and evaluation of copper based nanoparticles as agrochemicals against Phytophthora infestans', *RSC Advances*, 3(44), p. 21743. doi: 10.1039/c3ra42118j.

Gogos, A., Knauer, K. and Bucheli, T. D. (2012) 'Nanomaterials in Plant Protection and Fertilization : Current State , Foreseen Applications, and Research Priorities'.

Gottardo, S., Alessandrelli, M., Atluri, R., Barberio, G., Bergonzo, P., Bleeker, E., Andy, M., Borges, T., Buttol, P., Castelli, S., Chevillard, S., Dekkers, S., Delpivo, C., Fanghella, D. P., Dusinska, M., Einola, J., Ekokoski, E., Fito, C., Gouveia, H., Hoehener, K., Jantunen, P., Laux, P., Lehmann, H. C., Leinonen, R., Mech, A., Micheletti, C., Pesudo, L. Q., Polci, M. L., Walser, T., Wijnhoven, S. and Crutzen, H. (2017) *NANoREG framework for the safety assessment of nanomaterials*. doi: 10.2760/245972.

Grolimund, D. and Borkovec, M. (2005) 'Colloid-facilitated transport of strongly sorbing contaminants in natural porous media: Mathematical modeling and laboratory column experiments', *Environmental Science and Technology*, 39(17), pp. 6378–6386. doi: 10.1021/es050207y.

Hadley Wickham (2017) 'tidyverse: Easily Install and Load "Tidyverse" Packages'. Available at: https://cran.r-project.org/package=tidyverse.

Hooda, P. S. (2010) *Trace Elements in Soils*. Wiley-Blackwell. doi: 10.1002/9781444319477.

IAEA (2010) *Livechart - Table of Nuclides - Nuclear structure and decay data*, *Nuclear Data Sheets 111, 2425*. Available at: https://www-

nds.iaea.org/relnsd/vcharthtml/VChartHTML.html (Accessed: 12 October 2017).

Kah, M. (2015) 'Nanopesticides and Nanofertilizers: Emerging Contaminants or Opportunities for Risk Mitigation?', *Frontiers in Chemistry*, 3(November), pp. 1–6. doi: 10.3389/fchem.2015.00064.

Kah, M., Beulke, S., Tiede, K. and Hofmann, T. (2013) 'Nanopesticides: State of knowledge, environmental fate, and exposure modeling', *Critical Reviews in Environmental Science and Technology*, 43(16), pp. 1823–1867. doi: 10.1080/10643389.2012.671750.

Kah, M. and Hofmann, T. (2014) 'Nanopesticide research: Current trends and future priorities', *Environment International*. Elsevier Ltd, 63, pp. 224–235. doi: 10.1016/j.envint.2013.11.015.

von der Kammer, F., Ferguson, P. L., Holden, P. A., Masion, A., Rogers, K. R., Klaine, S. J., Koelmans, A. A., Horne, N. and Unrine, J. M. (2012) 'Analysis of engineered nanomaterials in complex matrices (environment and biota): General considerations and conceptual case studies', *Environmental Toxicology and Chemistry*, 31(1), pp. 32–49. doi: 10.1002/etc.723.

von der Kammer, F. Von Der, Legros, S. and Larsen, E. H. (2011) 'Separation and characterization of nanoparticles in complex food and environmental samples by field-flow fractionation', *Trends in Analytical Chemistry*. Elsevier Ltd, 30(3), pp. 425–436. doi: 10.1016/j.trac.2010.11.012.

Komárek, M., Čadková, E., Chrastný, V., Bordas, F. and Bollinger, J. C. (2010) 'Contamination of vineyard soils with fungicides: A review of environmental and toxicological aspects', *Environment International*, 36(1), pp. 138–151. doi: 10.1016/j.envint.2009.10.005.

Kookana, R. S., Boxall, A. B. A., Reeves, P. T., Ashauer, R., Beulke, S., Chaudhry, Q., Cornelis, G., Fernandes, T. F., Gan, J., Kah, M., Lynch, I., Ranville, J., Sinclair, C., Spurgeon, D., Tiede, K. and Van Den Brink, P. J. (2014) 'Nanopesticides: Guiding principles for regulatory evaluation of environmental risks', *Journal of Agricultural and Food Chemistry*, 62(19), pp. 4227–4240. doi: 10.1021/jf500232f.

Kretzschmar, R. and Sticher, H. (1997) 'Transport of humic-coated iron oxide colloids in a sandy soil: Influence of Ca2+ and trace metals', *Environmental Science and Technology*, 31(12), pp. 3497–3504. doi: 10.1021/es970244s.

Kühne, S., Strassemeyer, J., Roßberg, D., Kühne, S., Strassemeyer, J. and Roßberg, D. (2009) 'Anwendung kupferhaltiger Pflanzenschutzmittel in Deutschland', *Journal FR*

Kulturpflanzen, 61(4), pp. 126–130. Available at: http://www.ulmer-journals.de/ojs/index.php/jfk/article/download/57/65.

Laborda, F., Jiménez-Lamana, J., Bolea, E. and Castillo, J. R. (2011) 'Selective identification, characterization and determination of dissolved silver(i) and silver nanoparticles based on single particle detection by inductively coupled plasma mass spectrometry', *Journal of Analytical Atomic Spectrometry*, 26(7), p. 1362. doi: 10.1039/c0ja00098a.

Landwirtschaftliche Untersuchungs- und Forschungsanstalt, D. (2015) *Analyses Data Sheet for Standard Soils according to GLP*.

Lowry, G., Gregory, K., Apte, S. and Lead, J. (2012) 'Transformations of Nanomaterials in the Environment', *Frontiers of Nanoscience*, 7, pp. 55–87. doi: 10.1016/B978-0-08-099408-6.00002-5.

Lu, A., Zhang, S., Qin, X., Wu, W. and Liu, H. (2009) 'Aging effect on the mobility and bioavailability of copper in soil', *Journal of Environmental Sciences*. The Research Centre for Eco-Environmental Sciences, Chinese Academy of Sciences, 21(2), pp. 173–178. doi: 10.1016/S1001-0742(08)62247-0.

Ma, Y., Lombi, E., Oliver, I. W., Nolan, A. L. and McLaughlin, M. J. (2006) 'Long-term aging of copper added to soils', *Environmental Science and Technology*, 40(20), pp. 6310–6317. doi: 10.1021/es060306r.

Majedi, S. M. and Lee, H. K. (2016) 'Recent advances in the separation and quantification of metallic nanoparticles and ions in the environment', *TrAC - Trends in Analytical Chemistry*. Elsevier B.V., 75, pp. 183–196. doi: 10.1016/j.trac.2015.08.009.

Mavrocordatos, D., Pronk, W. and Boller, M. (2004) 'Analysis of environmental particles by atomic force microscopy, scanning and transmission electron microscopy', *Water Science & Technology*. doi: 50 (12) 9-18.

McCarthy, J. F. and Zachara, J. M. (1989) '"Subsurface Transport of Contaminants"', *Environmental Science and Technology*, 23(7), p. 752. doi: 10.1021/es00065a001.

McShane, H. V. A., Sunahara, G. I., Whalen, J. K. and Hendershot, W. H. (2014) 'Differences in soil solution chemistry between soils amended with nanosized CuO or Cu reference materials: Implications for nanotoxicity tests', *Environmental Science and Technology*, 48(14), pp. 8135–8142. doi: 10.1021/es500141h.

Mengel, K., Kirkby, E., Kosegarten, H. and Appel, T. (2001) *Principles of Plant Nutrition.*, *Soil Science*. doi: 10.1097/00010694-198407000-00012.

Navratilova, J., Praetorius, A., Gondikas, A., Fabienke, W., von der Kammer, F. and Hofmann, T. (2015) 'Detection of engineered copper nanoparticles in soil using single particle ICP-MS', *International Journal of Environmental Research and Public Health*, 12(12), pp. 15756–15768. doi: 10.3390/ijerph121215020.

Nowicki, W. and Nowicka, G. (1994) 'Verification of the Schulze-Hardy Rule: A Colloid Chemistry Experiment', *Journal of Chemical Education*, 71(7), p. 624. doi: 10.1021/ed071p624.

Pace, H. E., Rogers, N. J., Jarolimek, C., Coleman, V. A., Gray, E. P., Higgins, C. P. and Ranville, J. F. (2012) 'Single Particle Inductively Coupled Plasma-Mass Spectrometry: A Performance Evaluation and Method Comparison in the Determination of Nanoparticle Size', *Environmental Science & Technology*, 46(22), pp. 12272–12280. doi: 10.1021/es301787d.

Pace, H. E., Rogers, N. J., Jarolimek, C., Coleman, V. A., Higgins, C. P. and Ranville, J. F. (2012) 'Determining Transport Efficiency for the Purpose of Counting and Sizing Nanoparticles via Single Particle Inductively Coupled Plasma Mass Spectrometry (vol 83, pg 9361, 2011)', *Analytical Chemistry*, 84(10), p. 4633. doi: 10.1021/ac300942m.

Patnaik, P. (2003) *Handbook of Inorganic Chemicals*, *Ebook*. New York: McGraw-Hill. Available at: ftp://pvictor.homeftp.net/public/Sci_Library/Chem Library/Handbooks/Patnaik P. Handbook of inorganic chemicals (MGH, 2003)(T)(1125s).pdf.

Pauwels, H., Tercier-Waeber, M. Lou, Arenas, M., Castroviejo, R., Deschamps, Y., Lassin, A., Graziottin, F. and Elorza, F. J. (2002) 'Chemical characteristics of groundwater around two massive sulphide deposits in an area of previous mining contamination, Iberian Pyrite Belt, Spain', *Journal of Geochemical Exploration*, 75(1–3), pp. 17–41. doi: 10.1016/S0375-6742(01)00198-4.

R, C. T. (2016) 'R: A language and environment for statistical computing.' Vienna, Austria: R Foundation for Statistical Computing. Available at: https://www.r-project.org/.

Rao, C. R. M., Sahuquillo, A. and Sanchez, J. F. L. (2008) *A review of the different methods applied in environmental geochemistry for single and sequential extraction of trace elements in soils and related materials*, *Water, Air, and Soil Pollution*. doi: 10.1007/s11270-007-9564-0.

Rusjan, D. (2012) 'Copper in Horticulture', in D. Dhanasekaran, N. T. and A. P. (ed.)

Fungicides for Plant and Animal Diseases, pp. 257–278. Available at: http://cdn.intechopen.com/pdfs-wm/26033.pdf.

Rusjan, D., Strlič, M., Pucko, D. and Korošec-Koruza, Z. (2007) 'Copper accumulation regarding the soil characteristics in Sub-Mediterranean vineyards of Slovenia', *Geoderma*, 141(1–2), pp. 111–118. doi: 10.1016/j.geoderma.2007.05.007.

Salminen, R. (2005) *The geochemical atlas of Europe continent-wide distribution patterns of elements*, *Geochemical Atlas of Europe. Part 1: Background Information, Methodology and Maps*. Available at: http://weppi.gtk.fi/publ/foregsatlas/ (Accessed: 13 October 2017).

Servin, A., Elmer, W., Mukherjee, A., De la Torre-Roche, R., Hamdi, H., White, J. C., Bindraban, P. and Dimkpa, C. (2015) 'A review of the use of engineered nanomaterials to suppress plant disease and enhance crop yield', *Journal of Nanoparticle Research*, 17(2), pp. 1–21. doi: 10.1007/s11051-015-2907-7.

Shuman, L. M. (1991) 'Chemical forms of micronutrients in soils', *Micronutrients in agriculture*, (4), pp. 113–144. doi: 10.2136/sssabookser8.c5.

Sposito, G. (2008) *The Chemistry of Soils*. Second Edi. Oxford University Press.

Tan, K. H. (2010) 'Principles of soil chemistry / Kim H. Tan.', p. 560. Available at: http://encore.keele.ac.uk/iii/encore/record/C__Rb1544139__Ssoil__P0,4__Orightresult__U__X6?lang=eng&suite=cobalt.

Tegenaw, A., Tolaymat, T., Al-Abed, S., El Badawy, A., Luxton, T., Sorial, G. and Genaidy, A. (2015) 'Characterization and potential environmental implications of select Cu-based fungicides and bactericides employed in U.S. markets', *Environmental Science and Technology*, 49(3), pp. 1294–1302. doi: 10.1021/es504326n.

Thomas, R. (2001) 'TUTORIAL: A Beginner ' s Guide to ICP-MS (VI)', *Spectroscopy*, 16(October), pp. 44–48.

Tiede, K., Boxall, A. B. A., Tear, S. P., Lewis, J., David, H., Tiede, K., Boxall, A. B. A., Tear, S. P. and Lewis, J. (2008) 'Food Additives & Contaminants : Part A Detection and characterization of engineered nanoparticles in food and the environment', 49(October). doi: 10.1080/02652030802007553.

Tuoriniemi, J., Cornelis, G. and Hassellöv, M. (2012) 'Size discrimination and detection capabilities of single-particle ICPMS for environmental analysis of silver nanoparticles', *Analytical Chemistry*, 84(9), pp. 3965–3972. doi: 10.1021/ac203005r.

UN (2015) *Sustainable development goals - United Nations*, *2015*. Available at: http://www.un.org/sustainabledevelopment/sustainable-development-goals/ (Accessed: 11 October 2017).

Vogl, C. R. and Hess, J. (2016) *Organic farming in Austria*, *FEDERAL MINISTRY OF AGRICULTURE, FORESTRY, ENVIRONMENT AND WATER MANAGEMENT*. doi: doi:10.1017/S0889189300008274.

Weber, F.-A., Voegelin, A., Kaegi, R. and Kretzschmar, R. (2009) 'Contaminant mobilization by metallic copper and metal sulphide colloids in flooded soil', *Nature Geoscience*, 2(4), pp. 267–271. doi: 10.1038/ngeo476.

Xing, B., Vecitis, C. and Senesi, N. (2016) *Engineered Nanoparticles in the Environment*. Edited by B. Xing, C. Vecitis, and N. Senesi. Wiley-IUPAC Series in Biophysico-Chemical Processes in Environmental Systems.

Appendix

A. Test materials

Table A 1: Summary of test material (CuO NP and PPPs) properties. NPs based on these properties (assumptions R script) were detected during the initial characterization of CuO NP and Kocide suspension applying 5 sigma cut-off.

	CuO NPs	**Kocide**	**Cupravit**	**Bordeaux Mix**
Common name	Copper oxide NPs	Copper hydroxide	Copper Oxychloride	*Not assigned*
Chemical name	Copper(II) oxide or cupric oxide NPs	Copper (II) hydroxide	Dicopper chloride trihydroxide or Copper chloride hydroxide	*Not assigned*
Structural formula	CuO	$Cu(OH)_2$	$Cu_2Cl(OH)_3$	$CuSO_4 \cdot Ca(OH)_2 \cdot n\ H_2O$
Molecular weight [g/mol]	79,55	97,55	213,6	233,5 + n 18
Fraction Cu [%]	79,89	65,14	61,37	39,81 ($CuSO_4$)
Density [g/cm3]	6,32	3,37	3,6	3,6 ($CuSO_4$)
NP fraction detected (initial characterization)	✓	✓		

B. Initial characterization of Bordeaux and Cupravit (5 σ threshold)

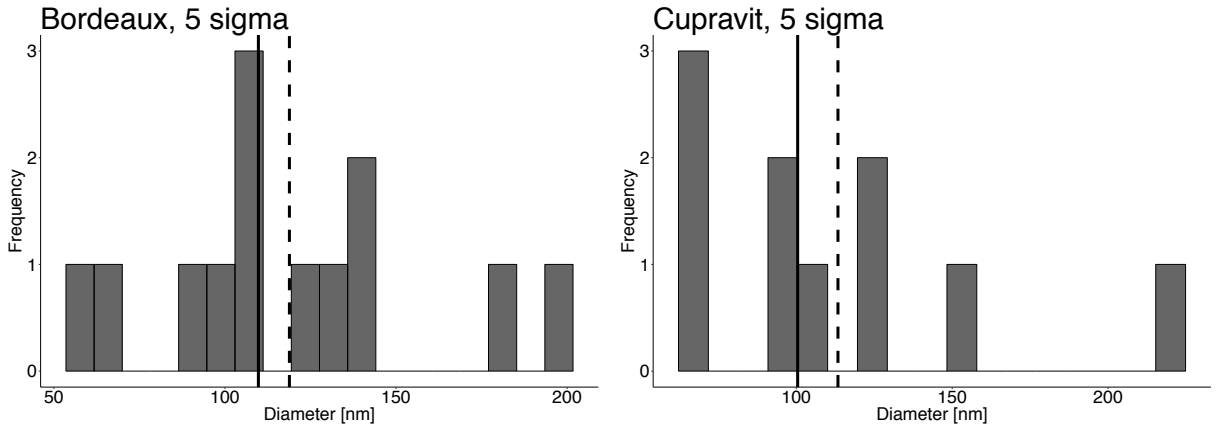

Figure A 1: Initial characterization of pristine Bordeaux and Cupravit suspension. In accordance with the ionic Cu control, particle frequencies from 0 - 5 are assumed to be artefacts from the dissolved signal. Hence, no NPs were detected in Bordeaux or Cupravit suspension using the 5σ threshold.

C. Bioavailable Cu concentrations

Table A 2: Bioavailable Cu concentrations obtained by the $CaCl_2$ extraction step. Mean values and Standard deviation (Std) are reported for each treatment type and measuring day (n = 3).

Day	**Blank control [mg kg^{-1}]**		**Ionic Cu control [mg kg^{-1}]**		**Bordeaux [mg kg^{-1}]**		**Cupravit [mg kg^{-1}]**		**Kocide [mg kg^{-1}]**		**CuO NP [mg kg^{-1}]**	
	Mean	*Std*	*Mean*	*Std*	*Mean*	*Std*	*Mean*	*Std*	*Mean*	*Std*	*Mean*	*Std*
0	0,02	0,00	1,77	0,05	1,17	0,02	1,22	0,05	1,31	0,03	0,07	0,00
2	0,02	0,00	0,62	0,03	0,56	0,02	0,70	0,08	0,59	0,00	0,15	0,01
4	0,01	0,00	0,46	0,02	0,44	0,02	0,50	0,02	0,48	0,04	0,16	0,02
8	0,01	0,00	0,43	0,02	0,37	0,03	0,42	0,01	0,45	0,06	0,22	0,00
14	0,02	0,00	0,49	0,01	0,51	0,06	0,55	0,06	0,57	0,01	0,34	0,02
21	0,02	0,00	0,67	0,01	0,53	0,01	0,74	0,01	0,70	0,02	0,48	0,01
31	0,01	0,00	0,78	0,09	0,63	0,06	0,86	0,07	0,76	0,05	0,49	0,04

D. Total Cu concentrations in colloidal extracts, summed 1 - 3

Table A 3: Total Cu extracted by the colloidal extraction steps using 1% FL70 solution. Values present mean values of total Cu (extraction 1 to 3 summed) and mean standard deviations (n = 3).

Day	**Blank control [mg kg^{-1}]**		**Ionic control [mg kg^{-1}]**		**Bordeaux [mg kg^{-1}]**		**Cupravit [mg kg^{-1}]**		**Kocide [mg kg^{-1}]**		**CuO NP [mg kg^{-1}]**	
	Mean	*Std*	*Mean*	*Std*	*Mean*	*Std*	*Mean*	*Std*	*Mean*	*Std*	*Mean*	*Std*
0	0,27	0,004	23,66	0,11	16,80	0,17	18,55	0,14	24,98	0,47	5,26	0,32
2	0,25	0,003	12,37	0,12	12,61	0,24	17,58	0,31	16,50	0,19	7,07	0,16
4	0,26	0,001	14,28	0,20	11,91	0,12	15,34	0,14	16,69	0,22	7,20	0,09
8	0,26	0,002	13,03	0,11	8,56	0,11	12,84	0,20	12,03	0,10	9,34	0,19
14	0,24	0,001	12,97	0,09	9,76	0,17	13,41	0,09	12,60	0,11	9,04	0,15
21	0,41	0,007	18,84	0,19	11,93	0,19	15,83	0,06	15,88	0,07	8,99	0,11
31	0,29	0,015	17,26	0,37	13,54	0,11	18,20	0,15	15,69	0,18	8,41	0,14

E. Total Cu in colloidal extracts

i. Blank control

Table A 4: Total Cu of blank control colloidal extracts 1 to 3, reported in mg Cu extracted per kg dry soil. Values present mean concentrations with standard deviation (Std) (n=3).

Day	**Extraction 1 [mg kg^{-1}]**		**Extraction 2 [mg kg^{-1}]**		**Extraction 3 [mg kg^{-1}]**	
	Mean	*Std*	*Mean*	*Std*	*Mean*	*Std*
0	0,111	0,010	0,082	0,002	0,076	0,002
2	0,083	0,004	0,081	0,003	0,087	0,001
4	0,089	0,002	0,074	0,000	0,093	0,002
8	0,092	0,003	0,081	0,002	0,084	0,001
14	0,098	0,001	0,075	0,002	0,068	0,001
21	0,139	0,004	0,119	0,004	0,151	0,011
31	0,128	0,004	0,091	0,005	0,072	0,036

ii. Ionic Cu control

Table A 5: Total Cu concentration of ionic control colloidal extracts 1 to 3, reported in mg Cu extracted per kg dry soil. Values present mean concentrations with standard deviation (Std) (n=3).

Day	**Extraction 1 [mg kg^{-1}]**		**Extraction 2 [mg kg^{-1}]**		**Extraction 3 [mg kg^{-1}]**	
	Mean	*Std*	*Mean*	*Std*	*Mean*	*Std*
0	10,50	0,03	8,48	0,26	4,69	0,12
2	4,65	0,28	4,14	0,05	3,58	0,13
4	5,47	0,48	4,44	0,14	4,37	0,14
8	5,41	0,30	3,91	0,07	3,72	0,04
14	6,07	0,16	3,81	0,01	3,09	0,19
21	7,35	0,15	4,92	0,07	6,57	0,50
31	8,52	0,59	4,60	0,28	4,14	0,54

iii. Bordeaux

Table A 6: Total Cu concentration of Bordeaux colloidal extracts 1 to 3 , reported in mg Cu extracted per kg dry soil. Values present mean concentrations with standard deviation (Std) (n=3).

Day	**Extraction 1 [mg kg^{-1}]**		**Extraction 2 [mg kg^{-1}]**		**Extraction 3 [mg kg^{-1}]**	
	Mean	*Std*	*Mean*	*Std*	*Mean*	*Std*
0	8,15	0,06	4,96	0,27	3,69	0,32
2	4,12	0,19	4,96	0,27	3,52	0,47
4	4,03	0,26	4,89	0,12	2,99	0,06
8	2,99	0,28	2,74	0,09	2,83	0,04
14	3,56	0,27	3,31	0,18	2,88	0,18
21	5,08	0,44	3,50	0,14	3,35	0,14
31	6,06	0,25	3,98	0,12	3,49	0,04

iv. Cupravit

Table A 7: Total Cu concentration of Cupravit colloidal extracts 1 to 3, reported in mg Cu extracted per kg dry soil. Values present mean concentrations with standard deviation (Std) (n=3).

Day	**Extraction 1 [mg kg^{-1}]**		**Extraction 2 [mg kg^{-1}]**		**Extraction 3 [mg kg^{-1}]**	
	Mean	*Std*	*Mean*	*Std*	*Mean*	*Std*
0	8,45	0,24	5,86	0,05	4,24	0,26
2	6,61	0,24	6,32	0,72	4,65	0,22
4	5,66	0,22	5,33	0,07	4,35	0,25
8	4,70	0,07	3,81	0,12	4,34	0,55
14	4,88	0,10	4,58	0,18	3,94	0,08
21	6,61	0,12	4,37	0,02	4,85	0,09
31	8,36	0,20	5,39	0,14	4,44	0,23

v. Kocide

Table A 8: Total Cu concentration of Kocide colloidal extracts (1-3), reported in mg Cu extracted per kg dry soil. Values present mean concentrations with standard deviation (Std) (n=3).

Day	**Extraction 1 [mg kg^{-1}]**		**Extraction 2 [mg kg^{-1}]**		**Extraction 3 [mg kg^{-1}]**	
	Mean	*Std*	*Mean*	*Std*	*Mean*	*Std*
0	11,7	0,8	8,1	0,4	5,2	0,6
2	5,6	0,3	6,6	0,3	4,3	0,1
4	5,9	0,3	7,0	0,3	3,9	0,3
8	4,3	0,2	3,8	0,1	3,9	0,1
14	4,8	0,2	4,1	0,1	3,7	0,1
21	7,1	0,1	4,4	0,1	4,4	0,1
31	6,9	0,5	4,8	0,1	3,9	0,1

vi. CuO NPs

Table A 9: Total Cu concentration of CuO NP colloidal extracts 1 to 3, reported in mg Cu extracted per kg dry soil. Values present mean concentrations with standard deviation (Std) (n=3).

Day	**Extraction 1 [mg kg^{-1}]**		**Extraction 2 [mg kg^{-1}]**		**Extraction 3 [mg kg^{-1}]**	
	Mean	*Std*	*Mean*	*Std*	*Mean*	*Std*
0	1,80	0,34	1,86	0,13	1,60	0,48
2	2,64	0,37	2,84	0,01	1,59	0,09
4	2,92	0,02	2,41	0,14	1,87	0,09
8	4,00	0,25	2,95	0,19	2,39	0,12
14	3,49	0,14	3,04	0,16	2,52	0,14
21	3,63	0,05	2,60	0,09	2,76	0,20
31	3,76	0,24	2,55	0,10	2,10	0,08

F. Bar chart diagrams of total Cu in colloidal extracts

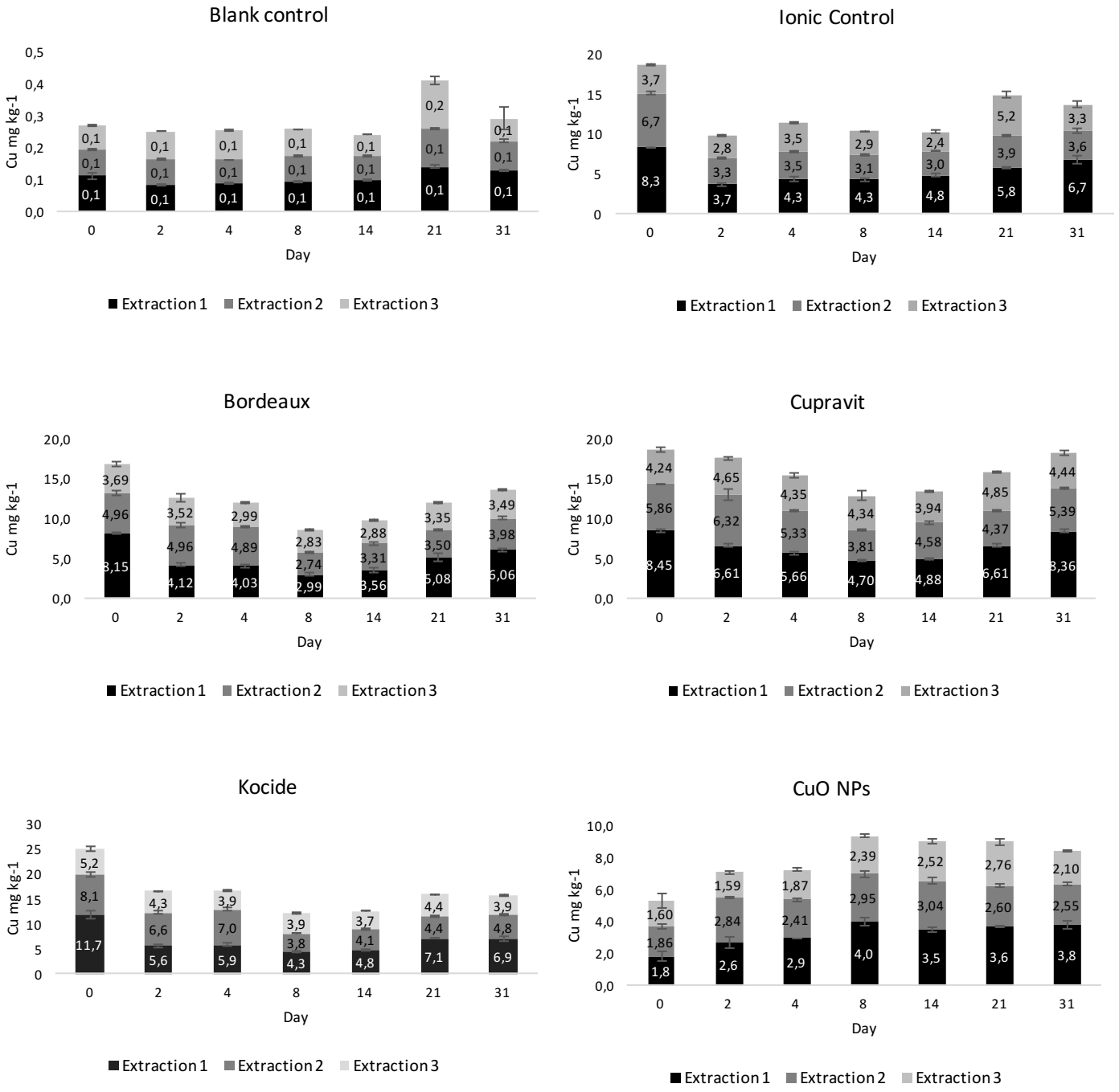

Figure A 2: Bar chart diagrams illustrating total Cu content of colloidal extracts (1-3) for each material (n = 3). Extraction 1 generally contains the largest total Cu fraction. Exceptions are CuO NP extracts on days 1 and 2, Kocide extracts on days 2 and 4 and Bordeaux on days 2 and 4. On these days extraction 2 contains more total Cu than extraction 1. Extracts 3 generally contain the smallest amounts of total Cu, except on day 21.

G. NP sizes

i. CuO NPs

Table A 10: Statistical summary of detectable NP sizes (applying 5 sigma) in colloidal extracts of CuO NP incubated standard soil.

CuO NPs	**Particle sizes [nm]**			
Day 0	*Extraction 1*	*Extraction 2*	*Extraction 3*	*Extraction 1-3*
Mean	125	99	99	106
Median	102	86	86	90
Std	80	51	52	61
Largest	565	421	375	565
Smallest	30	34	34	30
Day 2	*Extraction 1*	*Extraction 2*	*Extraction 3*	*Extraction 1-3*
Mean	100	87	90	96
Median	90	78	79	86
Std	45	39	43	44
Largest	332	259	301	332
Smallest	41	38	37	37
Day 4	*Extraction 1*	*Extraction 2*	*Extraction 3*	*Extraction 1-3*
Mean	85	95	83	87
Median	76	81	73	77
Std	38	51	40	43
Largest	298	377	287	377
Smallest	38	35	34	34
Day 8	*Extraction 1*	*Extraction 2*	*Extraction 3*	*Extraction 1-3*
Mean	101	90	90	94
Median	90	81	80	84
Std	46	40	41	42
Largest	355	308	338	355
Smallest	44	43	40	40
Day 14	*Extraction 1*	*Extraction 2*	*Extraction 3*	*Extraction 1-3*
Mean	97	63	66	75
Median	89	58	60	66
Std	42	25	27	36
Largest	347	213	240	347
Smallest	43	30	31	30

Day 21	*Extraction 1*	*Extraction 2*	*Extraction 3*	*Extraction 1-3*
Mean	75	73	90	78
Median	66	62	77	66
Std	31	34	47	37
Largest	225	238	378	378
Smallest	42	37	40	37

Day 31	*Extraction 1*	*Extraction 2*	*Extraction 3*	*Extraction 1-3*
Mean	133	99	75	109
Median	122	84	61	89
Std	62	47	42	54
Largest	309	267	264	309
Smallest	54	47	41	47

ii. Kocide

Table A 11: Statistical summary of detectable NP sizes (applying 5 sigma) in colloidal extracts of Kocide incubated standard soil.

Kocide	**Particle sizes [nm]**			
Day 0	*Extraction 1*	*Extraction 2*	*Extraction 3*	*Extraction 1-3*
Mean	156	144	128	143
Median	148	139	122	136
Std	47	43	34	44
Largest	450	397	350	450
Smallest	93	89	84	84

Day 2	*Extraction 1*	*Extraction 2*	*Extraction 3*	*Extraction 1-3*
Mean	122	126	106	120
Median	111	123	99	113
Std	43	31	29	38
Largest	318	230	224	318
Smallest	75	89	77	75

Day 4	*Extraction 1*	*Extraction 2*	*Extraction 3*	*Extraction 1-3*
Mean	97	95	70	90
Median	90	80	62	79
Std	34	69	26	47
Largest	270	1239	165	1239
Smallest	58	58	48	48

Day 8	*Extraction 1*	*Extraction 2*	*Extraction 3*	*Extraction 1-3*
Mean	94	95	75	91
Median	85	84	64	82
Std	36	68	32	35
Largest	250	1239	271	271
Smallest	55	53	48	53

Day 14	*Extraction 1*	*Extraction 2*	*Extraction 3*	*Extraction 1-3*
Mean	71	72	63	71
Median	64	69	58	65
Std	23	19	21	23
Largest	147	137	200	200
Smallest	48	48	41	48

Day 21	*Extraction 1*	*Extraction 2*	*Extraction 3*	*Extraction 1-3*
Mean	82	85	56	73
Median	79	65	52	64
Std	22	38	9	23
Largest	146	197	93	146
Smallest	58	51	48	48

Day 31	*Extraction 1*	*Extraction 2*	*Extraction 3*	*Extraction 1-3*
Mean	65	74	67	69
Median	62	57	62	62
Std	11	28	9	19
Largest	102	146	81	146
Smallest	56	55	55	55

H. Data processing script

The presented data processing script was substantial in treating the spICP-MS raw data in an objective and reproducible manner. The script consists of two parts: the main file “main.R” (i) and the file containing the data processing steps “functions.R” (ii). Both files belong to an R project named “myprogram.R”. First, basic a basic user guideline and then the program code are presented. Note that the filenames are exemplary.

Basic user instructions:

1. Set the working directory to the source file location (the folder in which myprogram.R or equivalent is contained)
2. Copy all necessary data into this folder for compactness
3. Create a new folder in the working directory and name it “input”
4. Copy the raw data of ONE material and ONE measuring day into the input folder (e.g. CuO NP measurements on day 0)
5. Adjust the assumed parameters in “functions.R” (e.g. for CuO NPs on day 0: fraction Cu = 0,8; density [fg/nm^3] = 6,3E-06; transport efficiency = slope = 185,55) and save
6. Run the program via executing “main.R”
7. After computing, a folder “output” will automatically be created and contain folders with the measurement names. These folders contain 2 subfolders for 3 and 5 sigma, respectively. Each sigma folder contains a graphical summary of the data, the NP intensities and NP sizes determined for the respective sigma value.

The code for this program is presented in the following section. Comments are preceded by “#” and green in color. The code itself is black.

i) Coding of file “main.R“

```
#This file executes functionsEXT.R, which contains all the data
reduction steps in the form of functions.
#The main file loops over all files contained in a folder called
"input"

library(tidyverse)
library(gridExtra)
source('functionsEXT.R') #required to read the functions
folder <- 'input'
```

```
folderlist <- list.files(folder)
#creates a list of what is contained in input folder

# test for one file only:
# filename <-  "merged/Day 00/Day 00 Kocide1 Ex1.csv"
# myfunction(filename)

# looping over the “Input” folder
for (subfolder in folderlist){

      foldername <- paste(folder, subfolder, sep='/')
#merges foldername and subfoldername seperated by / creating a string

      subfolderlist <- list.files(foldername, pattern='*.csv')
#creates a list of the .csv files contained in the subfolders(days)

      for (file in subfolderlist){

      filename <- paste(folder, subfolder, file, sep='/')

#creates a string that shows the folder (input), subfolder (day) and
file (sample), divided by "/"

      print(filename)
    myfunction(filename)

#use the function "myfunction" (as defined in functions.R) on
"filename" (= the individual measurements)
  }
}
```

ii) Coding of “functionsEXT.R”

```
# This file includes all required data reduction steps
# Additionally, it includes an input mask for the assumed material
properties and daily transport efficiency


############FUNCTIONS#############

# ITERATIVE OUTLIER TEST
# first mean of complete data set is determined, trimmed above n =
c(3,5) times sigma and new mean calculated. This is repeated until the
new mean = old mean

sigma_test <- function(data, n=3){
  # optional to set default sigma value
  # default sigma is applied if nothing defined in sigma_test
  # threeS <- mean + sd*3.0
  # number of sigmas applied
```

```
  data1 <- data #to avoid overwriting of the primary data
  mean <- mean(data1$intensity, na.rm = TRUE)
  sd <- sd(data1$intensity, na.rm = TRUE)

  max_iterations <- 1000

  for (i in 1:max_iterations)
  {
    inliers <- filter(data1, intensity <= mean + sd*n)
    mean_old <- mean
    mean <- mean(inliers$intensity)
    sd <- sd(inliers$intensity)
    if (mean == mean_old)
    {
      break
    }
  }

  threshold <- mean + sd*n
  inliers <- filter(data, intensity <= threshold)
  outliers <- filter(data, intensity > threshold)
  return(list(threshold=threshold, inliers=inliers, outliers=outliers))
}

# SUBSTRACT DISSOLVED BASELINE

subtract_baseline <- function(inliers, outliers){
      baseline <- mean(inliers$intensity, na.rm = TRUE)
      outliers$intensity <- outliers$intensity - baseline
      return(list(outliers=outliers, baseline=baseline))
}

# INTEGRATE PEAK SIZES (= "summing particle events")
# logic index to reduce noise contribution
# particles are assumed to appear in a particle "window" of at least 2
events
# particle events <2 are removed by "OR logic" statements: TRUE or
FALSE
# If two consecutive FALSE appear, the second value is removed from the
data

summing_events <- function(outliers){
  dwelltime <- outliers$time[3] - outliers$time[2]
  neighbour <- outliers

logic_index <- diff(outliers$time)<= dwelltime*1.1
  index <- logic_index
  for (i in 1:(length(logic_index)-1)){
    # print(logic_index[i] || logic_index[i+1])
    logic_index[i] <- logic_index[i] && logic_index[i+1]
  }
```

```
      neighbour <- neighbour[logic_index, ] #applies logic index to
      neighbour

#the "neighbouring" events describe the signals of one NP peak and are
summed up at this point

  for (i in 1:(nrow(neighbour)-1))
  {
    if (neighbour$time[i+1] - neighbour$time[i] <= dwelltime*1.1){
      neighbour$intensity[i+1] <- neighbour$intensity[i] +
neighbour$intensity[i+1]
      neighbour$intensity[i] <- 0
    }
  }

# FIRST RESULTS (dataframes within R)
  neighboursummed <- filter(neighbour, intensity > 0)
# intensities of NP peaks

  numberevents <- nrow(outliers)
# total number of signals above threshold

  numberparticles <- nrow(neighboursummed)
# total number of particles

  relparticlesize <- neighboursummed
  relparticlesize$intensity <- relparticlesize$intensity ^ (1.0/3.0)
# relative particle size = 3rd root of particle intensities

  return(list(neighboursummed=neighboursummed,
  numberevents=numberevents, numberparticles=numberparticles,
  relparticlesize=relparticlesize))
}

############MAIN FUNCTIONS#############

# DEFINING "MYFUNCTION"
# CREATE FILE NAMES BASED ON MEASUREMENT AND SIGMA VALUE APPLIED

myfunction <- function(filename){

  parts <- unlist(strsplit(filename, '/'))
  day <- parts[2]
  sample <- gsub('.csv', '', parts[3])
  #retrieves the sample names, substitutes the ending .csv with "space"

      data <- read_csv(filename, skip = 4, col_names = c('time',
      'intensity'))
      #skip lines with irrelevant content: skip = 1 in merged files;
      skip = 4 in original raw data files
      #in the main file "filename" will be consecutively replaced by the
      individual file paths
```

```
dwelltime <-data$time[3] - data$time[2]
#💡might be better to average all dwelltime differences to
minimize numeric errors..

data$intensity <- data$intensity*dwelltime
#convert [cnts/sec] to [cnts]

summary(data$intensity)
#returns statistical summary on data intensities

numberblockages <- filter(data, intensity == 0)
#gives the number of 0s registered = no signal (indicator for
instrumental blockages)

# APPLY N NUMBER X SIGMA
for (sigma in c(3,5)){

      sigmastring <- paste('sigma', sigma)
      foldername <- paste('output', day, sample, sigmastring,
      sep='/')
      dir.create(foldername, recursive = TRUE)
      #creates output folder which contains folders with day and
      sigma 3 and 5

      result <- sigma_test(data, n=sigma)
      #function sigma_test is defined above, works either way

      threshold <- result$threshold

      # print(result$outliers)
      result <- subtract_baseline(result$inliers, result$outliers)
      #function "substract_baseline" is defined above

      baseline <- result$baseline
      newthresh <- threshold - baseline
      # newthresh only for the plot
      # print(result$outliers)
      # print(result$baseline)

      result <- summing_events(result$outliers)
      # function "summing_events" is defined above
      print(result)
      neighboursummed <- result$neighboursummed
      # replace by data without baseline
      relparticlesize <- result$relparticlesize
      # sigma5 <- sigma_test(data, n=5)
```

```
####################SIZE CALIBRATION#####################################
slope <- 0.00 #transport efficiency, to be calibrated daily
fractionCu <- 0.00 #material specific
matdensity <- 0.00e-6 # 1 g/cm3 = 1 E-6 fg/nm3, material specific
#########################################################################

    correctionfactor <- slope
    massCu <- neighboursummed$intensity / correctionfactor
    massMat<- massCu / fractionCu
    Volume <- massMat / matdensity
    Radius <- (Volume/(4.0/3.0 * pi))^(1.0/3.0)
    Diameter <- 2.0*Radius

    DiameterDF <- data.frame(Diameter)
    summary(DiameterDF)
    meanS <- mean(DiameterDF$Diameter)
    medianS <- median(DiameterDF$Diameter)

     # GRAPHICAL SUMMARY
     plot1 <-    ggplot(data = data) +
                 geom_point(mapping = aes(x = time , y = intensity),
                 color = 'black', alpha = 0.8) +
                 ggtitle("Raw Data") +
                 geom_hline(aes(yintercept= baseline),
                 color= "#0072B2") +
                 geom_hline(aes(yintercept= threshold),
                 color="#009E78") +
                 labs( x = 'Time [s]', y = 'Frequency [cts] ')

     plot2 <-    ggplot(data = neighboursummed) +
                 geom_point(mapping = aes(x = time , y = intensity),
                 color="#009E73", alpha = 0.6 ) +
                 geom_hline(aes(yintercept= newthresh), color='black') +
                 ggtitle("Reduced Data") +
                 labs( x = 'Time [s]', y = 'Frequency [cts] ')

     p_hist1 <- ggplot(data = neighboursummed, aes(x = intensity)) +
                 ggtitle("Particle Intensity Distribution") +
                  geom_histogram(aes(y = ..count..), bins = 20, fill =
                 "#009E73", alpha = 0.6) +
                 #geom_line(stat='d' , colour= 'black', size = 1, alpha
                 = .6) +
                 labs( x = 'Intensity', y = 'Frequency')

     p_hist2<-  ggplot(data = DiameterDF, aes(x = Diameter)) +
                 ggtitle("Particle Size Distribution") +
                 geom_histogram(aes(y = ..count..), bins = 18, fill =
                 "#009E73", alpha = 0.6) +
                 geom_vline(aes(xintercept = meanS), colour="black",
                 linetype="dashed") +
                 geom_vline(aes(xintercept = medianS), colour="black") +
```

```
                #geom_line(stat='density' , colour= 'black', size = 1,
                alpha = .6) + #plots a density curve above histogram
                labs( x = 'Diameter [nm]', y = 'Frequency')+
                theme(axis.text=element_text(size=35),
                axis.title=element_text(size=35),
                title=element_text(size=38))

    g1 <- arrangeGrob(plot1, plot2, p_hist1, p_hist2, ncol=2, nrow=2,
          top = paste('sigma', sigma, sample))
    # creates an arrangement of 4 subplots in one graph

    ggsave(filename=paste(foldername, paste(sigma, 'sigma.png'),
    sep='/'), plot=g1)
    # saves the plot in the folder assigned to measurement and sigma
    value applied

    info <- data_frame(nrow(neighboursummed), threshold, baseline,
    meanS, medianS)
    # creates dataframe with relevant info for each measurement:
    Particle number, threshold, baseline intensity, mean and median
    size

    # SAVE RELEVANT DATA AS CSV FILES
    write.csv(info, file = paste(foldername, paste('sigma', sigma,
    sample, 'Info.csv'), sep='/'))
    # info file with summary

    write.csv(neighboursummed, file = paste(foldername, paste('sigma',
    sigma, sample, 'reduced.csv'),  sep='/'))
    # file with NP intensities [cnts]

    write.csv(relparticlesize, file = paste(foldername, paste('sigma',
    sigma, sample, 'Relparticlesize.csv'), sep='/'))
    # file with relative sizes (3rd square root of intensities)

    write.csv(DiameterDF, file = paste(foldername, paste('sigma',
    sigma, sample, 'Size.csv'), sep='/'))
    # file with equivalent sphere diameter
  }
}

#end
```